

Misalignment and Muon Scale Corrections Extracted from the 2011A $Z \rightarrow \mu\mu$ Sample

Arie Bodek, Jiyeon Han, and Willis Sakumoto

Department of Physics and Astronomy, University of Rochester, Rochester NY, 14627 USA

Abstract

We use the 2011A Drell-Yan $\mu^+\mu^-$ data sample in the Z Mass Region ($60 < M_{\mu\mu} < 120$ GeV/c²) to obtain corrections to the reconstructed muon momentum. These corrections, extracted using a new technique, compensate for misalignments of the CMS detector. We find that the misalignments in data and Monte Carlo are different and extract corrections for both samples. The samples used for the study correspond to 2.1 fb^{-1} of integrated luminosity collected in pp Collisions at $\sqrt{s}=7$ TeV till August, 22, 2011 (referred to as the 2011A data set). The corrections to the muon momentum in both data and MC, which we refer to as the Rochester Momentum Correction, are extracted as a function of muon charge (Q), η and ϕ . Different parameters to correct the reconstructed momentum in data and MC are available on line. We use this new technique because neither MusceFIT nor SIDRA fully correct for the misalignments in the data in the first 750 pb^{-1} of data (which is the only 2011 sample for which they are available). In addition, they are not available for the remainder of 2011A data or MC. Our correction can be obtained from the data in a couple of days after ntuples are made. Therefore, the extraction of the corrections for future data can be done quickly. In addition, we find that we need to add some additional smearing to the muon momentum in MC to match the data.

Version 3

1 Introduction

We use the 2011A Drell-Yan $\mu^+\mu^-$ data sample in the Z Mass Region ($60 < M_{\mu\mu} < 120 \text{ GeV}/c^2$) to obtain corrections to the reconstructed muon momentum to compensate for misalignments of the CMS detector. The samples used for the study correspond to 2.1 fb^{-1} of integrated luminosity collected in pp Collisions at $\sqrt{s}=7 \text{ TeV}$ till August, 22, 2011 (referred to as the 2011A data set). We use a new technique that has not been used before.

The CMS reconstruction software in both data and MC uses incorrect alignment geometries of the tracker. The misalignments in the data and the MC are different from each other. This affects the momentum determination of muons in both data and MC. The misalignment of the tracker results in a charge (Q), η , and ϕ dependence in the reconstruction of the muon momentum for both samples.

Although both data and MC samples were processed using the latest alignment geometry (as of December 2011) we find that the misalignment in the tracker is not fully accounted for. To correct for the remaining effect of misalignment, a CMS official momentum correction (MuscleFit) was developed by the tracking group. The MuscleFit correction is parametrized using Ansatz functions. The Ansatz functions should (in principle) correct for the residual charge, η , and ϕ dependence in the determination of the muon momentum. The functional forms are complicated and are different for data and MC.

The MuscleFit correction has been updated up to first 756 pb^{-1} of the 2011 data (though not approved yet and only extends to $\eta < 2.1$)[1]. When we apply the MuscleFit correction from the first 756 pb^{-1} to the 2011A (2 fb^{-1}) data, we find that it does not fully correct for misalignments (as described in an appendix to this note). When we apply the MuscleFit correction from the first 756 pb^{-1} only to the first 756 pb^{-1} of data, it still also does not fully correct for misalignments. There are no current plans to generate a MuscleFit for the full 2011A data set.

Also, there is no MuscleFit available for the 2011 MC set either (there are no current plan to generate a MuscleFit for the 2011 MC). We only have a MuscleFit for the 2010 MC. When we apply the 2010 MC MuscleFit to the 2011 MC, it also does a poor job.

In general we find that the MuscleFit partially corrects for misalignments in ϕ but does not correct for misalignments in η . In addition, it does not work above $\eta - 2.1$.

We understand why the MuscleFit does not work for $\eta > 2.1$ because that region was not used in the fit. It is not clear why the MuscleFit does not fully correct for the effects of misalignments for $\eta < 2.1$. The following are possible reasons:

- The MuscleFit uses functional forms for the corrections in η , ϕ and P_T which are too restrictive. It finds corrections for only three bins in η and only for $\eta < 2.1$
- The MuscleFit assumes a Breit Wigner for the Z Drell Yan data. However, the Z line shape is modified by final state radiation, EW interference (A_{FB}), by the P_T cut on the muon (acceptance), and by backgrounds. The line shape is correlated with the two η values for both muons and with the sign of the muon. Therefore using universal function for the Z line width will result in a bias in η which is different for positive and negative muon.

As shown in the appendix, we find similar conclusions for the SIDRA corrections.

In this note we use a new technique to extract corrections to the reconstructed muon momentum using the average of $1/p_T (< 1/p_T >)$ spectra of muons from Z decays. The basis of the method is the same as for the MuscleFit. Both our corrections and the MuscleFit corrections are extracted from the Z spectrum.

We use a fine grid in η and ϕ . Therefore, we are not constrained by a particular functional form. In addition, we include the effects of final state radiation, EW interference, and lepton P_T cut in the analysis for each η and ϕ bin. The corrections are extracted as a function of charge, in bins of η , and ϕ . In our method, there are no corrections between any of the η and ϕ bins. We will refer to this correction as the Rochester Momentum Correction.

The Rochester Momentum Correction corrects for all of the misalignments. Therefore, the Rochester Momentum Correction described in this note should be applied 2011A data without the application of any MuscleFit or SIDRA correction.

Although it is not really necessary, if MuscleFit or SIDRA are to be used in the analysis of data for some reason, we also provide an incremental Rochester momentum correction that corrects for residual misalignment which are not fully accounted for by either of these two methods. Since a MuscleFit for the 2011A MC has not been generated,

71 we do not provide an incremental correction for the 2011A MC. The only way to correct the 2011A MC is to use
72 the full Rochester correction.

73 2 Data Set and Event Selection

74 For the extraction of corrections to the reconstructed muon momentum we use 2011A data set which corresponds
75 to 2.1 fb^{-1} of integrated luminosity. We use events that pass the HLT DoubleMu_7 trigger path. The sample is
76 produced using the CMSSW_4_2_8 version. The Jason file is required to select the runs which satisfy the good
77 detector condition.

78 The MC sample that we use is the $Z \rightarrow \mu\mu$ POWHEG sample of Summer 11 version includes Pythia parton
79 showering. The analysis selection criteria are those proposed by the Vector Boson Task Force. as outlined in:
80 <https://twiki.cern.ch/twiki/bin/viewauth/CMS/VbtfZMuMuBaselineSelection>.

81 In the definition of isolation, we use the combined track and HCAL fractional isolation defined as $(TrkIso +$
82 $HadIso)_{\Delta R < 0.3} / P_T < 0.15$ (as used by the Dilepton group). If the EM energy is not included in the isolation
83 requirement, then the momentum dependence of the efficiency is expected to be constant. Therefore, we do not
84 include the EM energy in the definition of isolation.

85 Note that if the EM energy is included in the isolation requirement, then FSR photons cause in a momentum
86 dependence of the efficiency, as well as a complicated correlation between the efficiency of the two muons.

87 Specifically, the selection criteria are:

- 88 • HLT DoubleMu_7
- 89 • Muon selection : VBTF muon selection is applied
- 90 • $P_t > 20 \text{ GeV}$ and detector $|\eta| < 2.4$
- 91 • Global and Tracker Muon
- 92 • Combined relative isolation : $(TrkIso + HadIso)_{\Delta R < 0.3} / P_T < 0.15$
- 93 • Global muon normalized fit $\chi^2 < 10$
- 94 • Number of Tracker hits greater than 10
- 95 • Number of pixel hits greater than or equal to 1
- 96 • Number of muon stations greater than or equal to 2
- 97 • $dxy < 0.2$
- 98 • Mass selection : $60 < Mass < 120 \text{ GeV}/c^2$

99 The muon reconstruction efficiency as a function of η is extracted from the data. An efficiency scale factor obtained
100 from the data is applied to the MC to correct for the difference of the efficiency between data and MC.

101 3 Reference Plots Used in the Muon Momentum Study

102 A misalignment of the tracker generates distortions in several kinematic distributions of Drell-Yan ($Z/\gamma^* \rightarrow \mu\mu$)
103 events in the Z boson mass region. Since the misalignment of data and MC are different, the distributions will be
104 distorted in different ways for data and MC. Detector misalignment results in the following:

- 105 • It is responsible for charge (Q), η , and ϕ dependence of the reconstructed Z boson mass. (The expected Z
106 boson mass is known from the generated (post FSR with EW interference) spectrum in MC.)
- 107 • It yields difference in the overall shape of the dilepton mass distributions in the Z mass region between the
108 data and MC (if data and MC have different misalignments). A difference in shape could also occur if the
109 detector efficiency or resolution in the MC is not modeled correctly, or if the acceptance is not modeled
110 properly.

- 111 • A charge dependence in the reconstructed muon momentum creates unphysical wiggles in the forward and
112 backward charge asymmetry (A_{fb}) of Drell-Yan events as a function of dilepton mass (in the region of the
113 Z peak). This yields one of two powerful checks on a difference in the momentum scale between positive
114 and negative muons.
- 115 • In the low Z boson P_T region ($P_T < 10 \text{ GeV}/c$), the ϕ distribution in the Collins-Soper frame (CS) [4],
116 ϕ_{CS} , is expected to be flat. However, resolution smearing in the muon momentum creates an excess around
117 $\phi_{CS} = 0$ and $\pm\pi$ in the reconstructed ϕ_{CS} . The level of the excess at $\phi_{CS} = 0$ and $\pm\pi$ is expected to
118 be the same if the muon momentum scales and resolutions are the same between μ^+ and μ^- . Therefore,
119 ϕ_{CS} distribution in low Z P_T region provides the second powerful check on a difference in the momentum
120 scale between positive and negative muons. A simple way to think about this is as follows: ϕ_{CS} is the angle
121 between the direction of the Z boson P_T and the direction of the positive lepton. For Z $P_T = 0$ there is no
122 preferred x axis. However, if the calibration of the positive and negative muons are different, $P_T = 0$ events
123 end up with a Z P_T along either the positive or the negative muon direction in ϕ_{CS}

124 In our study we use the following kinematic distributions as reference plots to test the validity of the momentum
125 corrections. These reference plots are not used in the extraction of the momentum corrections. They are only used
126 to ascertain that the correction factors actually work.

- 127 • The overall dimuon invariant mass spectrum ($M_{\mu^+\mu^-}$).
- 128 • A_{fb} as a function of mass.
- 129 • ϕ_{CS} in two Z P_T bins: $0 < P_T < 5 \text{ GeV}/c$, and $5 < P_T < 10 \text{ GeV}/c$.
- 130 • A comparison of the Z P_T spectrum between data and MC.
- 131 • The average Z mass as a function of ϕ of the μ^+ , or the μ^- (and also the mass with no sign requirement.)
- 132 • The average Z mass as a function of η of the μ^+ , or the μ^- (and also the mass with no sign requirement.)
- 133 • We use the same procedure to extract the corrections for data and MC. Since for the MC we know the
134 generated muon momentum, we can use the generated information in the MC sample as an additional check
135 on the procedure.

136 Figure 1 and 2 show the reference plots before the application of any muon momentum correction to either data or
137 MC. The Z boson has the forward and backward asymmetry (A_{fb}), which results on the asymmetry in the Z mass
138 profile plot for μ^- and μ^+ . This effect is shown in the plot in the right side of Figure 3 (black vs. red points).

139 Figure 3 shows the Z mass profile in $60 < M < 120 \text{ GeV}/c^2$ mass range as a function of μ^- and μ^+ in
140 the generator level but after photon radiation (post FSR) for the ideal case of full acceptance, and no resolution
141 smearing (i.e. a perfect detector). The red curve in Figure 1 and 2 are those expected for such a perfect detector.
142 The P_T spectrum used in these plots are uncorrected POWHEG predictions. We know from the 2010 data that the
143 POWHEG predictions do not agree with data and need to be tuned.

144 Generator plots which include the effects of FSR, resolution smearing, acceptance, and with the correct P_T spec-
145 trum for the real CMS detector, but with perfect alignment are shown in Fig. 4 and 5. These will be used later in
146 iteration 2

147 The following features are observed in Fig. 1:

- 148 • The top two plots indicate that the location of the Z peak in mass is incorrect and the shape of the data in
149 mass is different from the MC.
- 150 • The left middle plot shows unphysical wiggles in A_{fb} in both data and MC, indicating that the momentum
151 scales for positive and negative muons are different in both data and MC. This can only originate from a
152 misalignments in both data and MC.
- 153 • The right middle plot shows that the MC does not have the correct P_T spectrum.
- 154 • The bottom two plots show that the MC does not have the correct P_T spectrum (level) and that the momentum
155 scales for positive and negative muons are different (the peaks at $\phi_{CS} = 0$ and $\pm\pi$ have different heights).

156 The following features are observed in Fig. 2:

- 157 • The top two plots show that the average Z mass ($60 < M < 120 \text{ GeV}/c^2$) depends on the ϕ of the positive
158 and negative muon (it should be independent of ϕ). They also show that the momentum scales for positive
159 and negative muons are different in both data and MC, and the difference is a function of ϕ of the muon.
- 160 • The bottom two plots show that the η dependence of average Z mass ($60 < M < 120 \text{ GeV}/c^2$) for positive
161 and negative muons in data and MC are different.

162 4 Muon Momentum Correction- First Iteration

163 To correct for the effect of track misalignments, we extract a correction to the reconstructed muon momentum
164 which is a function of charge (Q), η , and ϕ of the muon as a first iteration.

165 The procedure is to require that the mean of $1/p_T$ ($< 1/p_T >$) of muons in data (reconstructed) and MC (recon-
166 structed) in bins of Q , η , and ϕ should each be equal to the mean $< 1/p_T >$ of the MC at the generated level (in a
167 specific Q , η , and ϕ bin).

168 Since the Z mass is known, and the P_T spectrum in MC can be tuned to agree with the data (though this is a small
169 effect) this procedure should in principle an absolute calibration of the momentum scale. For iteration 1, we use
170 the generated means for a perfect detector with perfect resolution acceptance and alignment. (Later, for iteration 2
171 we will use generated information the effect of resolution smearing, the effect of P_T cut on the spectrum, but with
172 perfect alignment).

173 In general, an overall momentum scale (e.g. error in the B field) should be the same for positive and negative
174 muons. A misalignment would results in a difference in the mean $< 1/p_T >$ between positive and negative muon.
175 A muon momentum correction portion that corrects for a misalignment is additive in $1/p_T$. A muon momentum
176 correction portion to correct for wrong BdL is multiplicative and is the same for positive and negative muons.
177 In our procedure, we extract both the additive and multiplicative part of the corrections. We do not account for
178 possible errors in dE/dx (material). For these, we assume that these are done correctly, since the amount of material
179 is known (they also have a negligible effect on muons in the Z mass region).

180 The correction factor, $C^{Data/MC}(Q, \eta, \phi)$, is defined as the difference in the mean $< 1/p_T >$ between the mean
181 $< 1/p_T >$ for the MC at the generated level and reconstructed data (or reconstructed MC). This is done in bins of
182 Q , η and ϕ .

183 The correction factors $C^{Data/MC}(Q, \eta, \phi)$ for positive and negative muons are the regrouped to form two different
184 corrections

- 185 • A muon momentum scale multiplicative correction D_m that could originate from an incorrect integral of
186 $B \cdot dL$.
- 187 • An additive bias correction D_m that could originates from misalignment.

188 The muon momentum scale correction D_m that may originate from an incorrect integral of $B \cdot dL$ does not depend
189 on the sign of the charge dependence. Its $1/p_T$ dependence is corrected as a multiplicative correction.

190 The muon momentum correction D_a that may originate from misalignment depends on the charge of the muon.
191 The correction hs opposite signs for μ^+ and μ^- . Its $1/p_T$ dependence is corrected as an an additive correction.

192 In addition, we define an overall scale correction G which is determined by the known Z mass peak position. At
193 this stage G will not be equal to 1 because we used the generated information for a perfect detector with perfect
194 resolution, full acceptance and perfect alignment for the expect mean of $1/p_T$. (Later, for iteration 2 we will use
195 generated information the effect of resolution smearing, the effect of P_T cut on the spectrum, but with perfect
196 alignment. For iteration 2, we expect G to be 1.0)

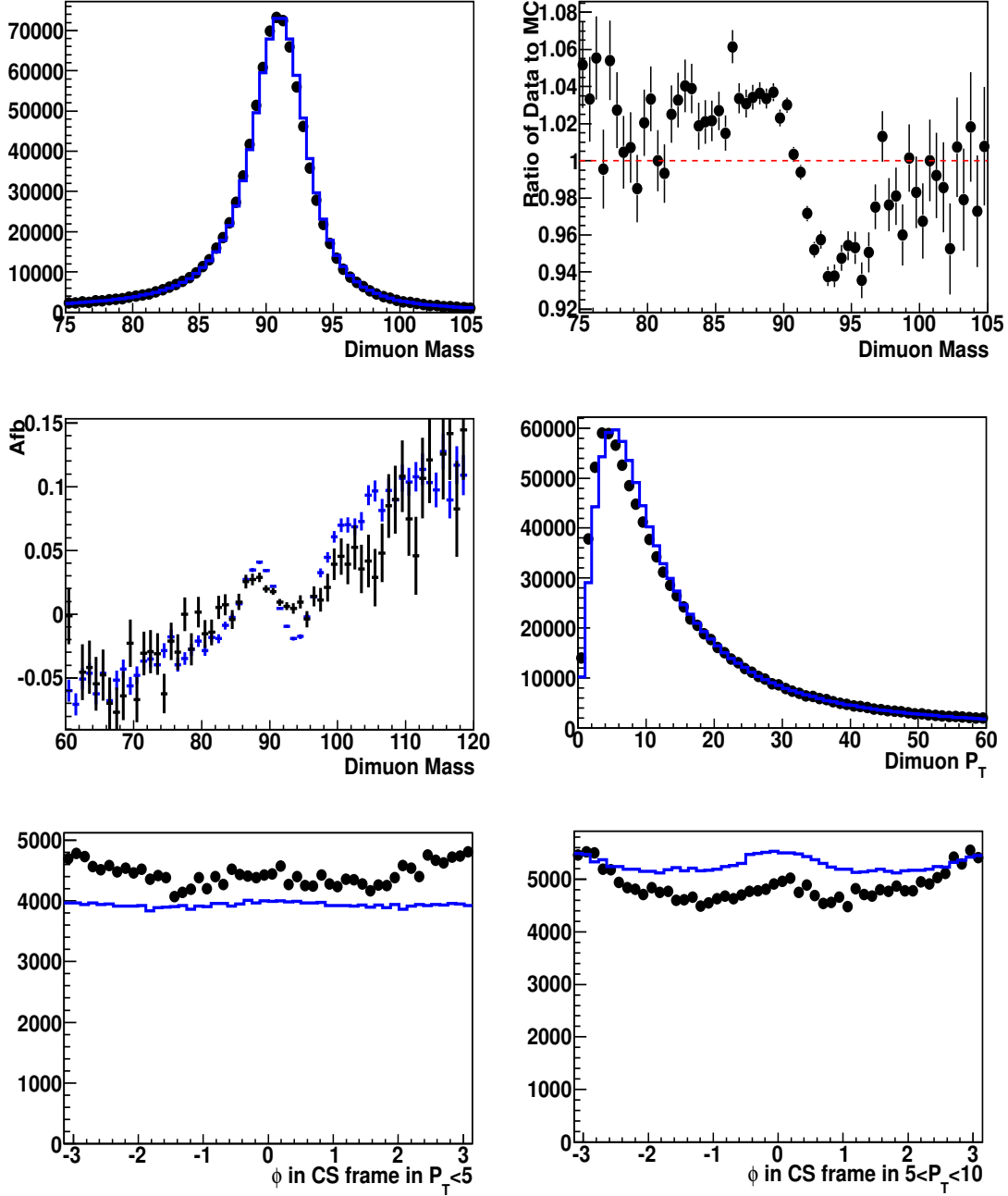


Figure 1: 2011A (2.1 fb^{-1}) reference plots (page 1) BEFORE any corrections. Top Plots: Comparison of the dimuon invariant mass distribution between the data (black) and MC (blue) (left), and the ratio of data to MC (right). Middle plots: Comparison of A_{fb} as a function of mass (left) and boson P_T distribution (right) between the data (black) and MC (blue). Bottom plots: Comparison of ϕ in the Collins-Soper frame for boson $P_T < 5 \text{ GeV}/c$ (left), and ϕ in the Collins-Soper frame for boson $5 < P_T < 10 \text{ GeV}/c$ (right) for data (black) and MC (blue). The plots are normalized to the total number of events of the data in the $60 < M_{\mu\mu} < 120 \text{ GeV}/c^2$ mass range. (a) The top two plots indicate that the location of the Z peak in mass is incorrect and the shape of the data in mass is different from the MC. (b) The left middle plot shows unphysical wiggles in A_{fb} in both data and MC, indicating that the momentum scales for positive and negative muons are different in both data and MC (c) The right middle plot shows that the MC does not have the correct P_T spectrum. (d) The bottom two plots show that the MC does not have the correct P_T spectrum (level) and that the momentum scales for positive and negative muons are different (the peaks at $\phi_{CS} = 0$ and $\pm\pi$ are different).

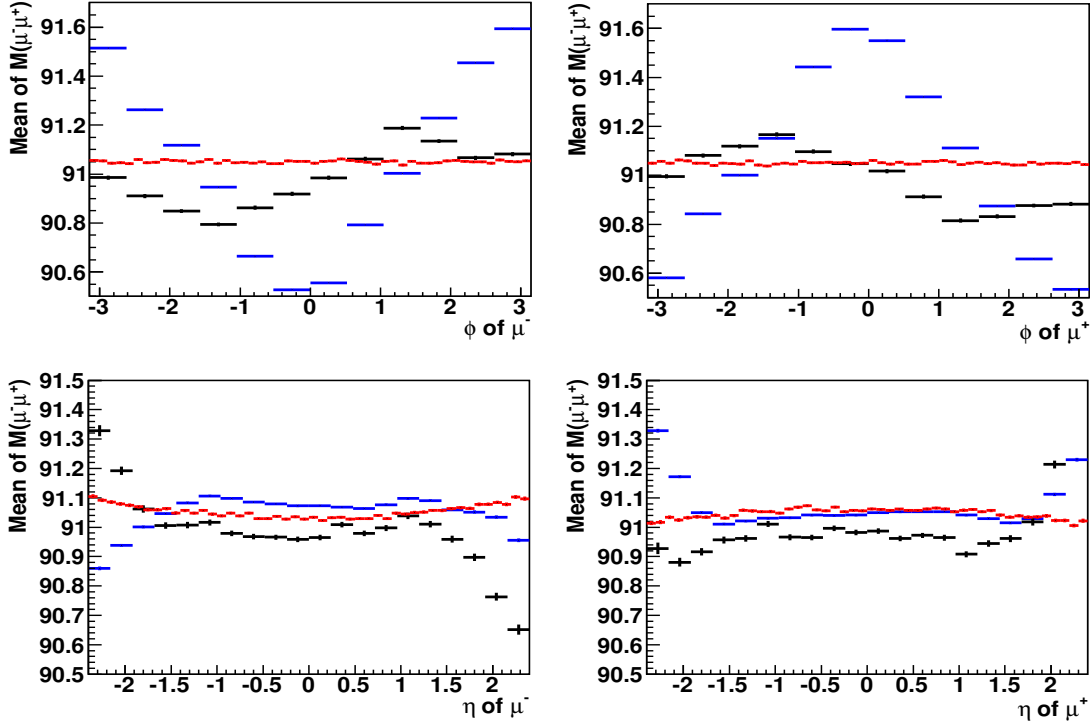


Figure 2: 2011A (2.1 fb^{-1}) reference plots (page 2) BEFORE any corrections: Top Plots: Comparison of the average of $M_{\mu\mu}$ as a function of ϕ for μ^- (left) and the average of $M_{\mu\mu}$ as a function ϕ for μ^+ (right) between the data (black) and MC (blue). Bottom Plots: Comparison between the data (black) and MC (blue) of the average of $M_{\mu\mu}$ as a function of η for μ^- (left) and the average of $M_{\mu\mu}$ as a function of η for μ^+ (right). The top two plots show that the average Z mass depends on ϕ (it should be independent of ϕ). They also show that the momentum scales for positive and negative muons are different in both data and MC, and the difference is a function of ϕ of the muon. The bottom two plots show that the η dependence of the muon momentum scales in data and MC are different. The average of $M_{\mu\mu}$ is obtained in the tight mass window, $86.5 < M_{\mu\mu} < 96.5 \text{ GeV}/c^2$. The red points are $M_{\mu\mu}$ profile plot in the generator level after final state radiation (FSR) for a perfect detector. These perfect detector curves do yet include detector smearing effects, or P_T cut, and do not use tuned P_T distributions). The plots including these effects (for iteration 2) are shown in Fig. 4 and 5.

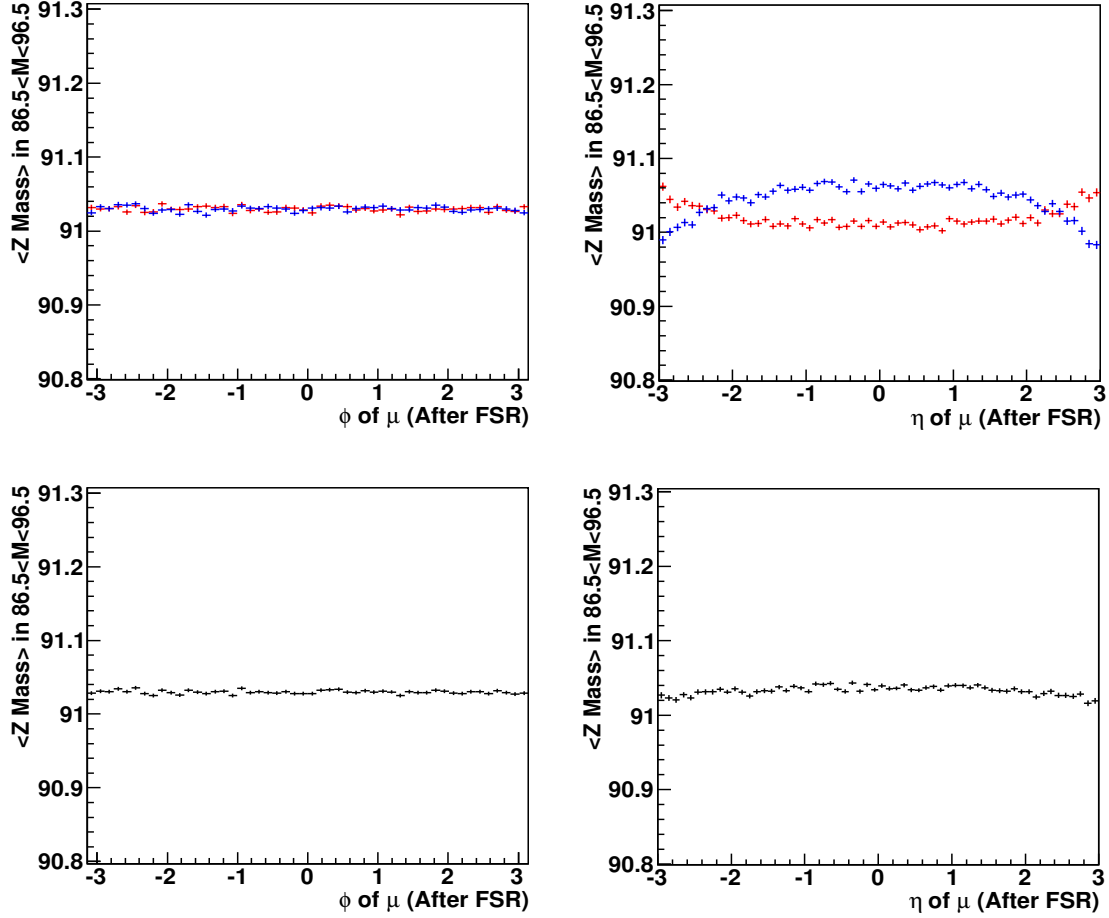


Figure 3: Generator level plots for a perfect detector with full acceptance, perfect resolution, and perfect alignment. Shown are the Z mass profile plot as a function of ϕ (left) and η (right) of μ in the generator level. Top plot : Average Z mass ($86.5 < M < 96.5 \text{ GeV}/c^2$) as a function of ϕ (left) and η (right) of μ^- (red points) and μ^+ (blue points) in the generator level without any selection after the photon radiation effect (FSR). There is a different in the average mass for positive and negative muons because of the electroweak forward-backward asymmetry. Bottom plot : Average Z mass ($86.5 < M < 96.5 \text{ GeV}/c^2$) as a function of ϕ (left) and η (right) of μ with no separation between positive and negative muons (black points) in the generator level without any selection after the photon radiation effect (FSR). The tight mass window, $86.5 < M < 96.5 \text{ GeV}/c^2$, is used to get the mean of the Z mass ($y - axis$). Note, this perfect detector plot does include the effect of resolution smearing , or P_T cut on muons, or tuning of P_T distributions. The plots including these effects (for iteration 2) are shown in Fig. 4 and 5).

$$C^{Data/MC}(Q, \eta, \phi) = \langle 1/p_T^{MC(gen.)}(Q, \eta, \phi) \rangle - \langle 1/p_T^{Data/MC(rec.)}(Q, \eta, \phi) \rangle \quad (1)$$

$$D_m(\eta, \phi) = (C^{Data/MC}(+, \eta, \phi) + C^{Data/MC}(-, \eta, \phi))/2.0 \quad (2)$$

$$D_a(\eta, \phi) = (C^{Data/MC}(+, \eta, \phi) - C^{Data/MC}(-, \eta, \phi))/2.0 \quad (3)$$

$$\frac{1}{p_{T,\eta,\phi:corrected}^\pm} = \frac{1}{p_T^\pm} \times (1.0 + D_m(\eta, \phi) / \langle 1/p_T^\pm \rangle) \pm D_a(\eta, \phi) \quad (4)$$

$$p_{T,scale+\eta,\phi:corrected}^\pm = G \times p_{T,\eta,\phi:corrected}^\pm \quad (5)$$

197 where, MC(rec.) and MC(gen.) denote the muon momentum for the MC at the reconstructed and generated levels,
 198 respectively. The $C^{Data/MC}$ is the muon momentum correction factor for the data or MC in bins of Q , η , and ϕ
 199 of the muon (8×8 matrix in η and ϕ for each muon polarity). This $\langle 1/p_T \rangle$ correction corrects for the charge, η ,
 200 and ϕ dependence of the mis-reconstructed momentum, as well as an overall scale to yield the correct Z mass. As
 201 discussed in the text, G is expected to be different from 1.0 for iteration 1 (but not for iteration 2).

202 Figure 6 and 7 show the $\langle 1/p_T \rangle$ correction for the data and for the MC ($C^{Data/MC}(Q, \eta, \phi)$).

203 After the application of the the multiplicative and additive corrections, the Z peak position at the reconstructed
 204 level in data and MC are tuned with a multiplicative corrections G^{data} and G^{MC} to agree with the generated level
 205 after FSR, which is 91.06 GeV/c² after kinematic cuts ($P_T > 20$ GeV and $|\eta| < 2.4$ for both muons). That peak
 206 position is obtained by fitting the generated spectrum (post FSR) in a narrow Z mass region (88 to 94 GeV) to a
 207 Breit-Wigner function.

208 The Z mass peak positions for the reconstructed data and reconstructed MC (both after the application of additive
 209 and multiplicative momentum correction are also obtained by fitting the distributions in a narrow Z mass region
 210 (88 to 94 GeV) to a Breit-Wigner function.

211 In addition, the resolution in the Monte Carlo does not match the resolution in data. The parameters Δ , and SF,
 212 are estimated by comparing the overall $M_{\mu+\mu-}$ mass distributions between data and MC (using a χ^2 test). These
 213 parameters are only applied to the MC. They are define by the following equations (which are also used at CDF):

$$\frac{1}{p_T^{additional-smearing}} = \frac{1}{p_T} + \Delta \times Random :: Gaus(1, SF) \quad (6)$$

214 where p_i is the reconstructed muon momentum in MC ($i = x, y, \text{ and } z$) and $p_i^{gen.}$ is the generated muon momentum
 215 in MC.

216 Figure 8 shows χ^2 distributions for the comparison of data to MC as a function of the values of each global scale
 217 factor. The measured global factors (extracted from the χ^2 plot) are summarized in Table 1.

Table 1: Iteration 1: The parameters Δ , and SF are additional resolution smearing parameters (Δ , and SF) to be applied to the MC. These parameters are determined by comparing the $M_{\mu+\mu-}$ distributions in data and MC. The global scale factors G^{data} and G^{MC} are used to set the Z peak position at the correct place.

Global Factor	Value
Δ	$(-3.8549 \pm 0.7880) \times 10^{-6}$
SF	33.4858 ± 0.4899
G^{data}	1.0020 ± 0.0001
G^{MC}	1.0005 ± 0.0001

218 Figure 9 shows the reference plots after applying the iteration 1 correction factors, $C(Q, \eta, \phi)$, G to both data
 219 and MC (and Δ , and SF to the MC). The reference plots show better agreement between the data and MC. The
 220 unphysical wiggles in the A_{fb} distributions in both data and MC are no longer there, and the peaks at $\phi_{CS} = 0$
 221 and $\pm\pi$ are of equal magnitude. However, the middle plot shows that Z P_T distribution in MC do not agree with
 222 the data. This results in offsets between data and MC in the ϕ_{CS} distributions for the two Z P_T ranges. (The
 223 distributions are normalized to the total number of events in data for $60 < M_{\mu+\mu-} < 120$ GeV/c² mass window.)

224 The disagreement [6] between data and MC for the $Z P_T$ distribution at low P_T implies that the POWHET MC
 225 generator with Pythia parton showering (used in CMS) should be tuned. In order to get better agreement between
 226 the data and MC, we apply a $Z P_T$ correction shown in Figure 10 to the MC at the generator level such that it
 227 matches the data. This $Z P_T$ correction is in agreement with the ratio of the published $Z P_T$ distributions in 2010,
 228 and the POWHEG prediction (also show in the figure).

229 The $Z P_T$ correction removes the discrepancy in the overall levels in the comparison of ϕ_{CS} distributions between
 230 the data and MC for the two low P_T ranges. Figure 11, 12, and 13 show the reference plots after applying both
 231 the momentum correction and the additional $Z P_T$ correction in MC. With the additional $Z P_T$ correction, there is
 232 agreement in the overall level in ϕ_{CS} distributions between data and MC. After all correction, we compare the p_T
 233 distribution of μ^- and μ^+ between data and MC (shown in Figure 14.)

Table 2: Iteration 2: The parameters Δ , and SF are additional resolution smearing parameters (Δ , and SF) to be applied to the MC. These parameters are determined by comparing the $M_{\mu^+\mu^-}$ distributions in data and MC. The global scale factors G^{data} and G^{MC} are used to set the Z peak position at the correct place. For iteration 2, we expect the values of G to be very close to 1.0.

Global Factor	Value
Δ	$(-3.0409 \pm 0.7682) \times 10^{-6}$
SF	43.4069 ± 1.5054
G^{data}	1.0009 ± 0.0001
G^{MC}	1.0000 ± 0.0001

234 5 Muon Momentum Correction- Iteration 2

235 Now that the $Z P_T$ in the Powheg MC generator has been tuned to match the data, we repeat our analysis, and
 236 extract updated muon momentum corrections.

237 This is the second iteration. In iteration 2 we make sure that the mean $1/P_T$ in generated (post FSR) distributions
 238 for each η and ϕ bins is corrected for resolution smearing and the P_T cut on the samples. This is done by applying
 239 an η dependent gaussian smearing to the generated (post FRST) muon momentum to account for the detector
 240 resolution and applying a P_T . The mean of $1/P_T$ is changed by resolution smearing and by the P_T cut. We now
 241 have the means of $1/P_T$ for a perfectly aligned detector which has the resolution and acceptance of the CMS
 242 detector. Figure 15 shows the η dependent resolution of the muon momentum which was determined from a
 243 SIDRA study. [2]. We also apply the kinematic selection, muon $p_T > 2t$ GeV/c and $|\eta| < 2.4$ for both muons
 244 in the generator post FSR level to make sure that the acceptance for the generated events is the same as data.
 245 (The $\langle 1/p_T \rangle$ muon correction factors in iteration is obtained in the range of $1/p_T < 0.04$) With these two
 246 corrections, the mean $1/P_T$ as a function of η and ϕ for these generated events is what should be expected both in
 247 Data and MC if there is no bias in the momentum scale or misalignment.

248 Figure 4 and 5 show the reference plots for the generated post FSR sample after applying both corrections. This
 249 is what we expect both the data and the MC to look like after all biases and misalignments are corrected with our
 250 muon corrections.

251 Figure 16 and 17 show the $\langle 1/p_T \rangle$ muon correction factors for the data and MC in iteration 2. The momentum
 252 corrections for iteration 2 are close to the corrections extracted in the first iteration.

253 Figure 8 shows the χ^2 distribution for the global factors, Δ , and SF, for iteration 2. The global factors Δ , SF,
 254 and G for iteration 2 are given in Table 2. The generated Z mass peak after FSR with the eta dependent gaussian
 255 smearing is 90.9956 ± 0.0015 GeV/ c^2 and the data and MC is matched to have the same Z mass peak using the
 256 global factor, G. For this iteration the values of G are expected to be close to 1.0.

257 Figure 19, 20, and 21 show the reference plots after all corrections for iteration 2, and Figure 22 shows the p_T
 258 distribution of the muon after all corrections for iteration 2.

259 6 Iteration 3

260 This iteration is yet to be done. . As expected, the global scale factor for the MC after iteration 2 is 1.0000 ± 0.0001
 261 (which is an error of 0.0090 GeV, or 9 MeV). Note that the MC does not have any background.

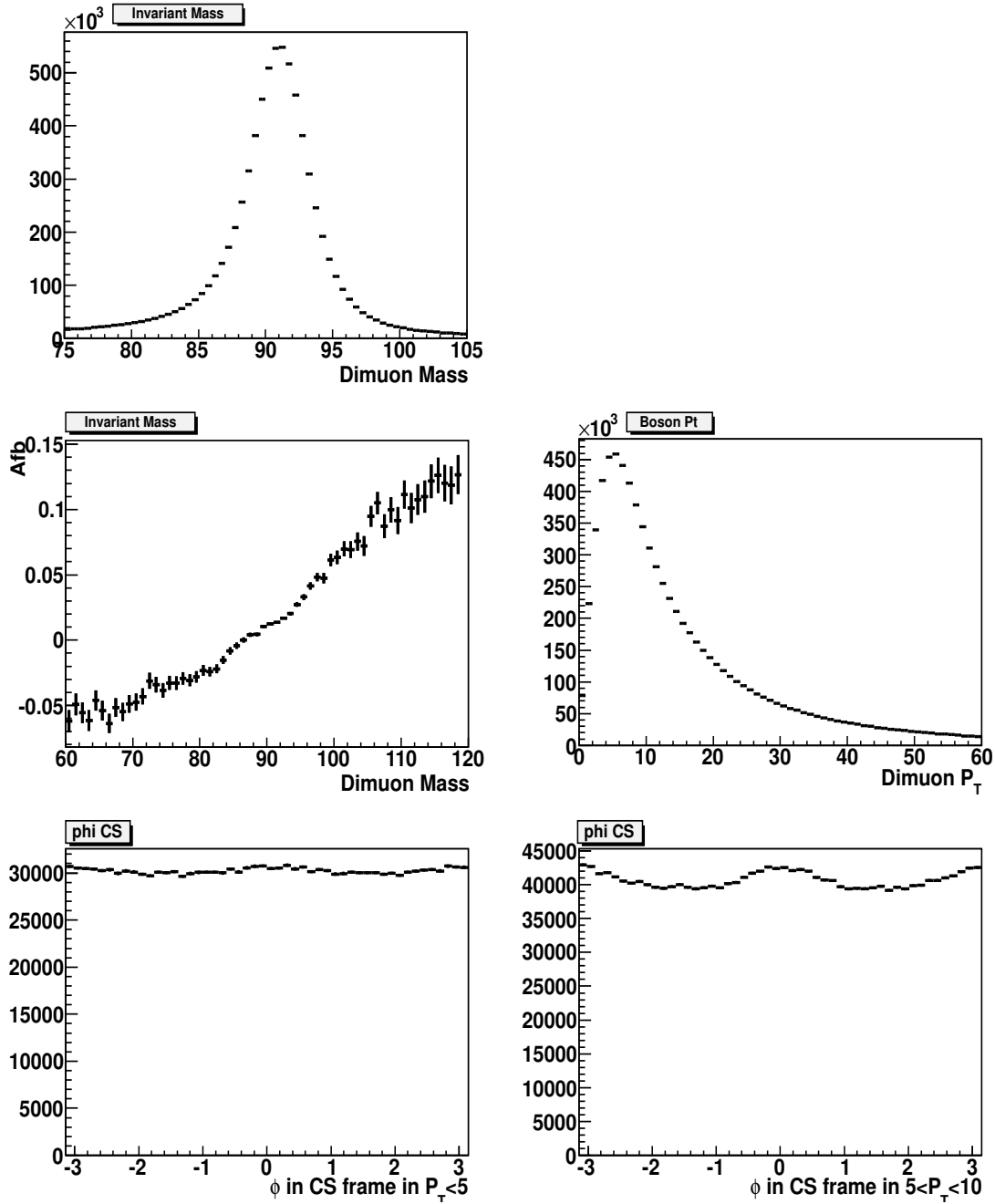


Figure 4: Expected reference plots after all corrections (page 1). Shown are the reference plots ($M_{\mu^+\mu^-}$, A_{fb} , $Z P_T$, and ϕ_{CS}) in the generator level after applying the eta dependent detector resolution smearing effect with the kinematic selection, muon $p_T > 20$ GeV/c and $|\eta| < 2.4$ for both muons and tuning the P_T distributions in POWHEG (which is a small effect). Top Plots: The dimuon invariant mass distribution. Middle plots: A_{fb} (left) and boson P_T (right) distributions. Bottom plots: The ϕ distribution in the Collins-Soper frame in boson $P_T < 5$ GeV/c (left) and ϕ in the Collins-Soper frame in boson $5 < P_T < 10$ GeV/c (right) distributions.

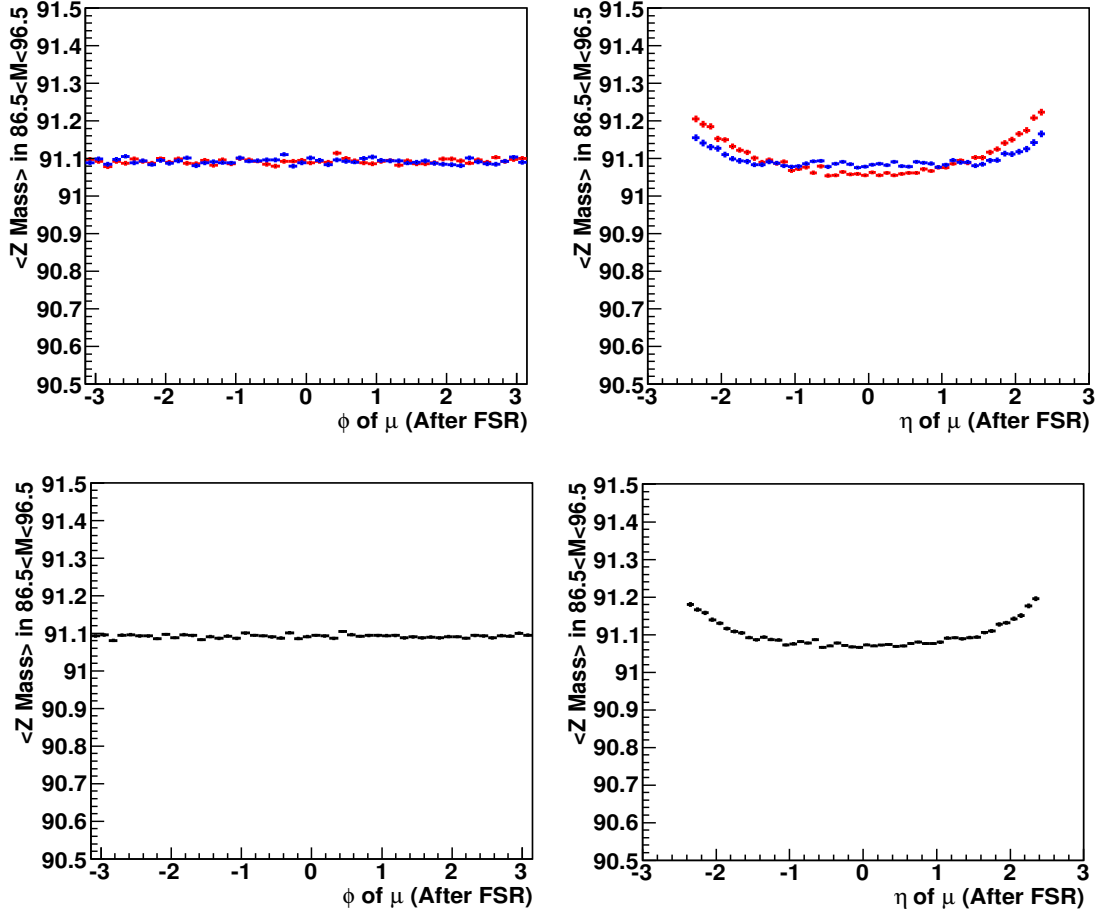


Figure 5: Expected reference plots after all corrections (page 2). Shown are the reference plots for Z mass profile plot as a function of ϕ (left) and η (right) of μ in the generator level after applying the η dependent detector resolution smearing effect with kinematic selection i.e. muon $p_T > 20$ GeV/c and $|\eta| < 2.4$ for both muons (and tuning the P_T distributions in POWHEG which is a small effect). Top plot : Average Z mass ($86.5 < M < 96.5$ GeV/c²) as a function of ϕ (left) and η (right) of μ^- (red points) and μ^+ (blue points) in the generator level after the photon radiation effect (FSR). There is a difference in the average mass for positive and negative muons because of the electroweak forward-backward asymmetry. However, the overall η dependence comes from the $p_T > 20$ GeV/c cut. Bottom plot : Average Z mass ($86.5 < M < 96.5$ GeV/c²) as a function of ϕ (left) and η (right) of μ with no selection in the charge of muons (black points) in the generator level after the photon radiation effect (FSR). The tight mass window, $86.5 < M < 96.5$ GeV/c², is used to get the mean of the Z mass (y -axis).

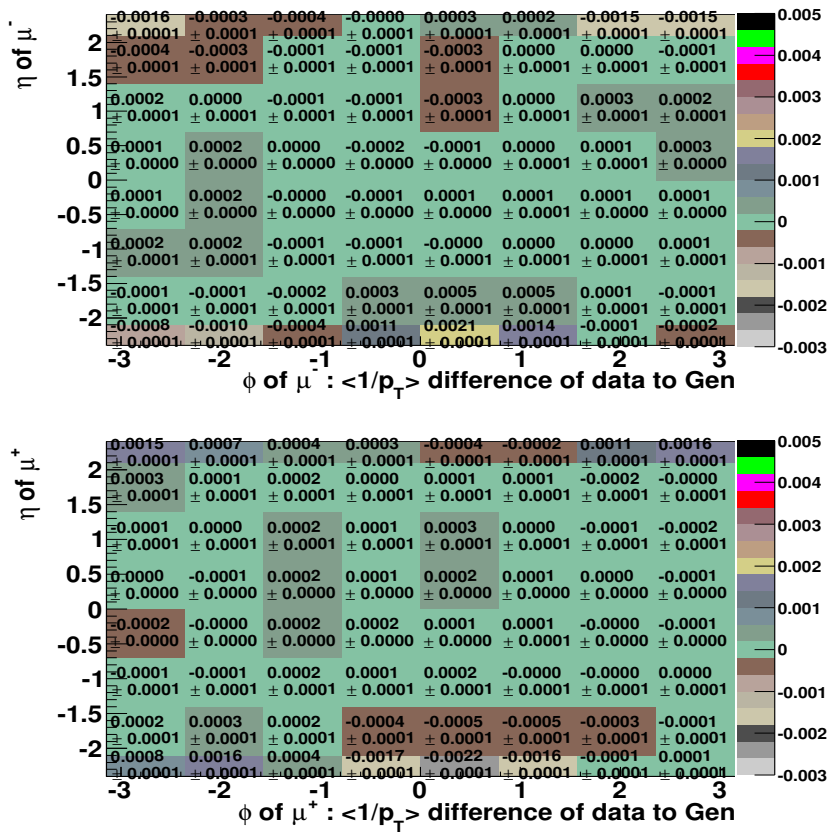


Figure 6: Iteration 1 for the 2011A (2 fb^{-1}) data: The $\langle 1/p_T \rangle$ correction for data for μ^- (top) and μ^+ (bottom) in η and ϕ (for iteration 1).

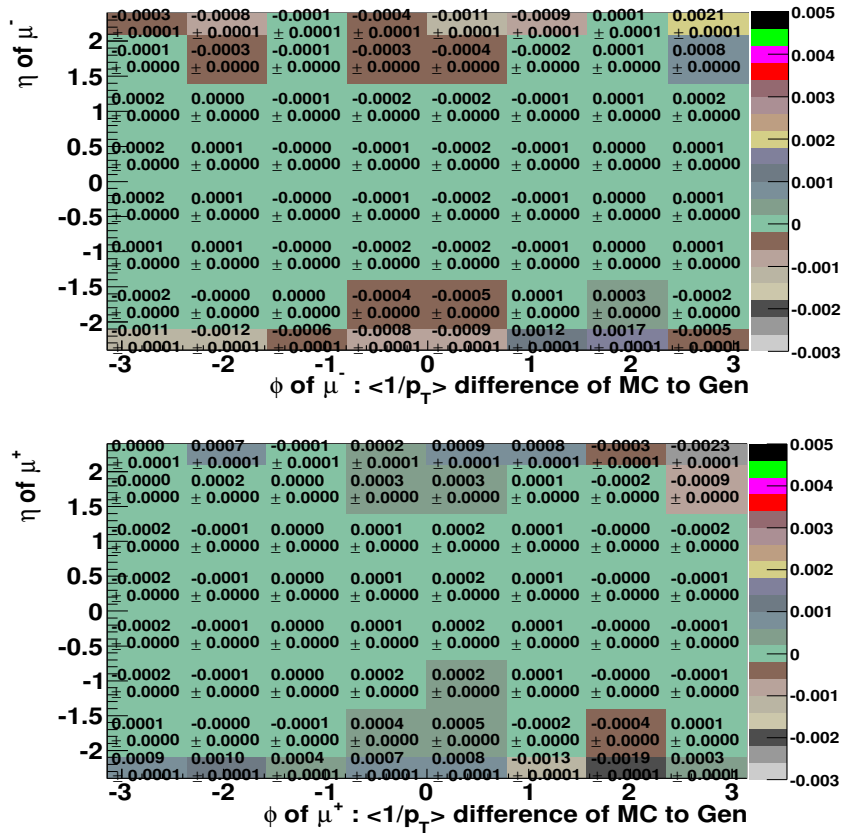


Figure 7: Iteration 1 for the 2011A (2 fb^{-1}) MC: The $\langle 1/p_T \rangle$ correction for MC for μ^- (top) and μ^+ (bottom) in η and ϕ .

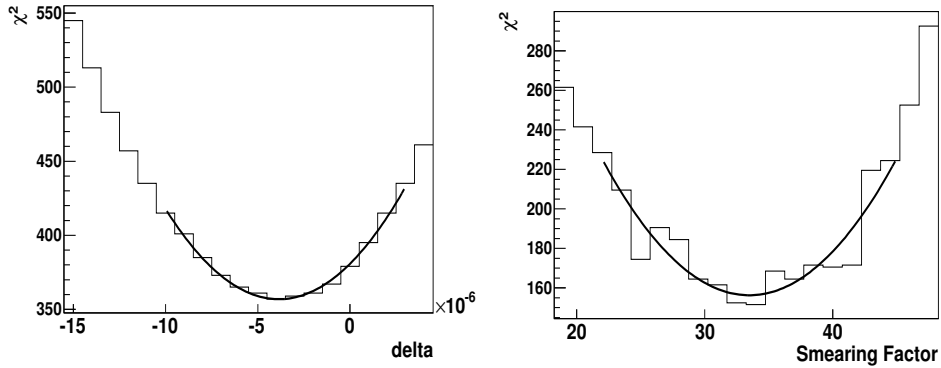


Figure 8: Iteration 1 for the 2011A (2 fb^{-1}): χ^2 distribution as a function of the global factor, Δ (left) and SF (right).

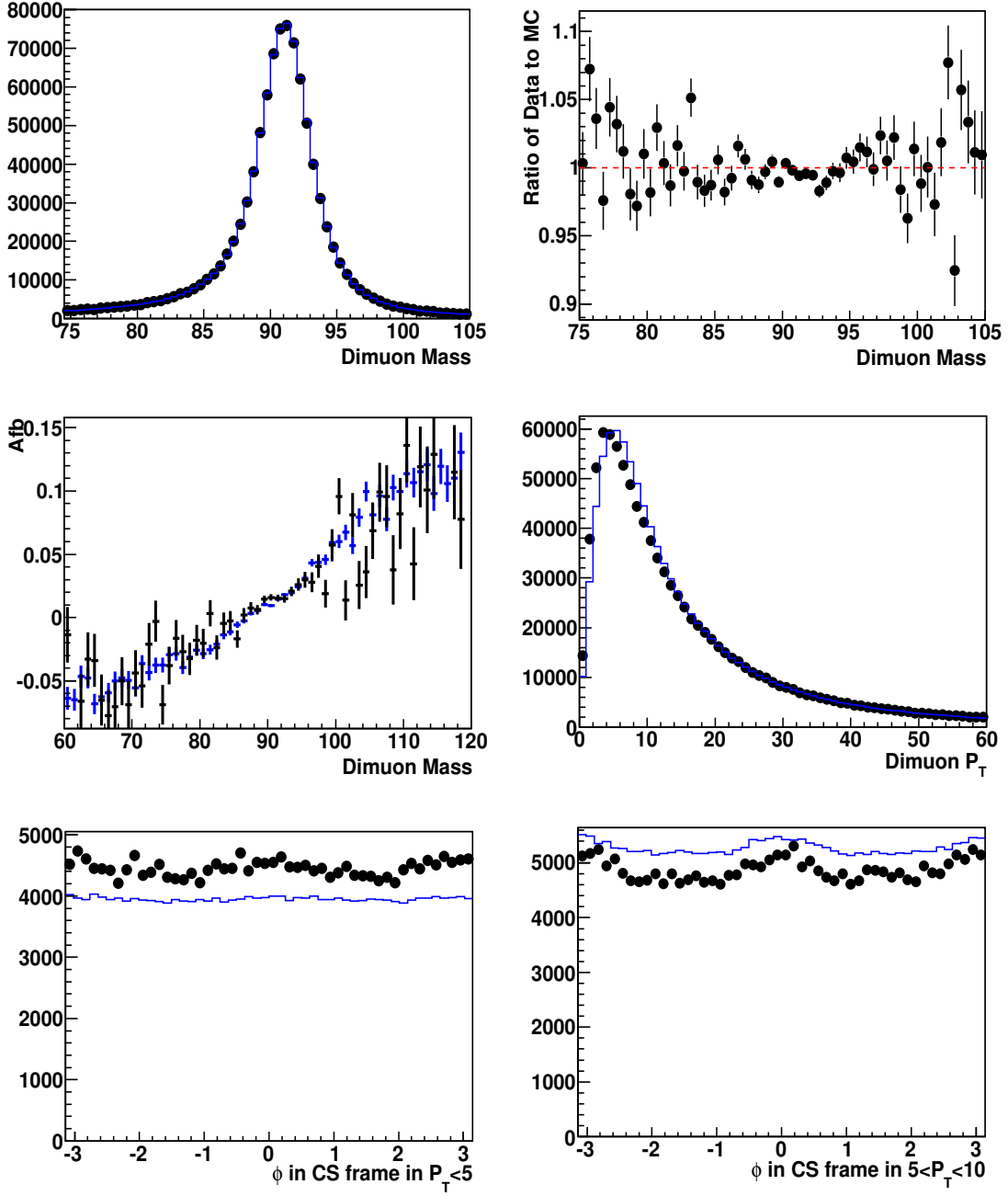


Figure 9: Iteration 1 for the 2011A (2 fb^{-1}) data : The reference plots ($M_{\mu^+\mu^-}$, A_{fb} , $Z P_T$, and ϕ_{CS}) after the application of the iteration 1 muon momentum correction. Top Plots: Comparison of the dimuon invariant mass distribution between the data (black) and MC (blue) (left) and its ratio of data to MC (right). Middle plots: Comparison of A_{fb} (left) and boson P_T (right) distributions between the data (black) and MC (blue). Bottom plots: Comparison of ϕ in the Collins-Soper frame in boson $P_T < 5 \text{ GeV}/c$ (left) and ϕ in the Collins-Soper frame in boson $5 < P_T < 10 \text{ GeV}/c$ (right) distributions between the data (black) and MC (blue). The plots are normalized to the total number of events of the data in $60 < M_{\mu\mu} < 120 \text{ GeV}/c^2$.

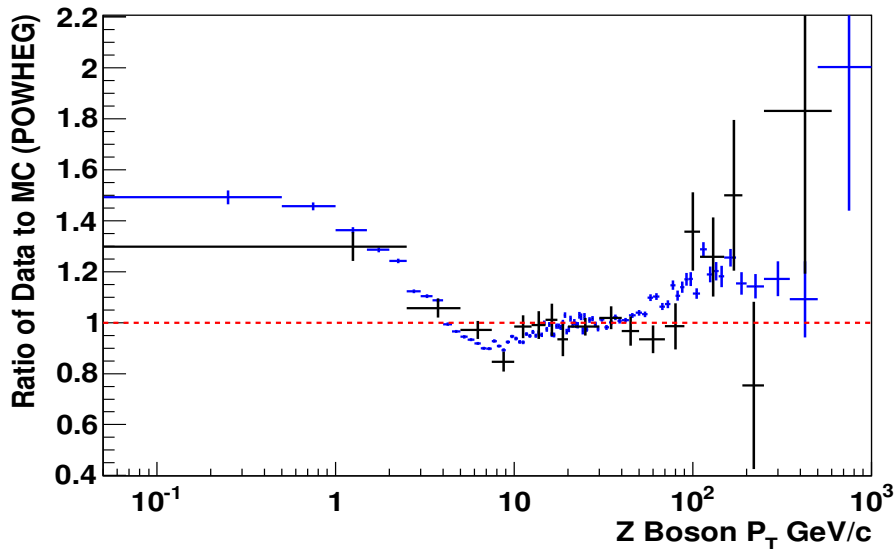


Figure 10: The $Z P_T$ correction applied to the MC at the generated level. The correction factor is obtained by comparing $Z P_T$ spectrum between the data and MC after iteration 1 for 2011A (2 fb^{-1}). Also shown are the ratios of the P_T spectrum published for the 2010 data divided by the POWHEG prediction in the generator level. Our $Z P_T$ correction to the POWHEG MG generator is in agreement with the CMS 2010 measurement.

262 The scale factor for iteration 2 for the data is 1.0009 ± 0.0001 (a shift of 90 MeV with an error of 10 MeV). This
 263 shift could be due to the fact that we did not account for the background in the data.

264 In iteration 3, we will correct for the small QCD, EW (diboson), $\tau^+\tau^-$ and top-antitop background to the sample
 265 for the data. A comparison of the dimuon spectrum of the data, with MC, showing the level of the background, is
 266 shown in Figure??.

267 We will correct for the shift in the mean $1/P_T$ from background for each ϕ and η .

268 Therefore, the corrections that we have now after iteration 2, have a systematic error of about 100 MeV, or 0.1%
 269 in the overall scale.

270 7 Conclusion

271 Using the Drell-Yan dimuon sample, we extract corrections to the reconstructed muon momentum that originate
 272 from tracking misalignments. The corrections are obtained by using the average $\langle 1/p_T \rangle$ of muon in bins of
 273 charge, η , and ϕ in conjunction with the dimuon invariant mass distributions. Corrections are extracted for both
 274 data and MC.

275 The $M_{\mu^+\mu^-}$, A_{fb} , ϕ_{CS} distributions are used as reference plots to test the procedure. After the application of
 276 the muon momentum correction, the reconstruction bias which is a function of charge, η , and ϕ is removed. All
 277 kinematic distributions which are used as reference plots show good agreement between the data and MC. The
 278 offline code for the muon momentum corrections (referred to as the Rochester Momentum Correction) is now
 279 available online.

280 At this stage we estimate the systematic error in the correction with iteration 2 correction factor at $\pm 0.1\%$ (which
 281 corresponds to an error of 100 MeV in the Z peak).

282 Analysis such as dilepton A_{FB} , and the W asymmetry are sensitive to differences in the momentum scales between
 283 positive and negative muons. For such analysis, the use of the Rochester correction makes a significant difference.
 284 For other analyses such as the P_T spectrum of Z bosons, it may be less significant. Figure ?? shows the ratio of
 285 the P_T distribution for Z bosons of data after correction with the Rochester correction, or MuscleFit correction or
 286 SIDRA correction to the data before any corrections for the 2011A (2.1 fb^{-1}) sample.

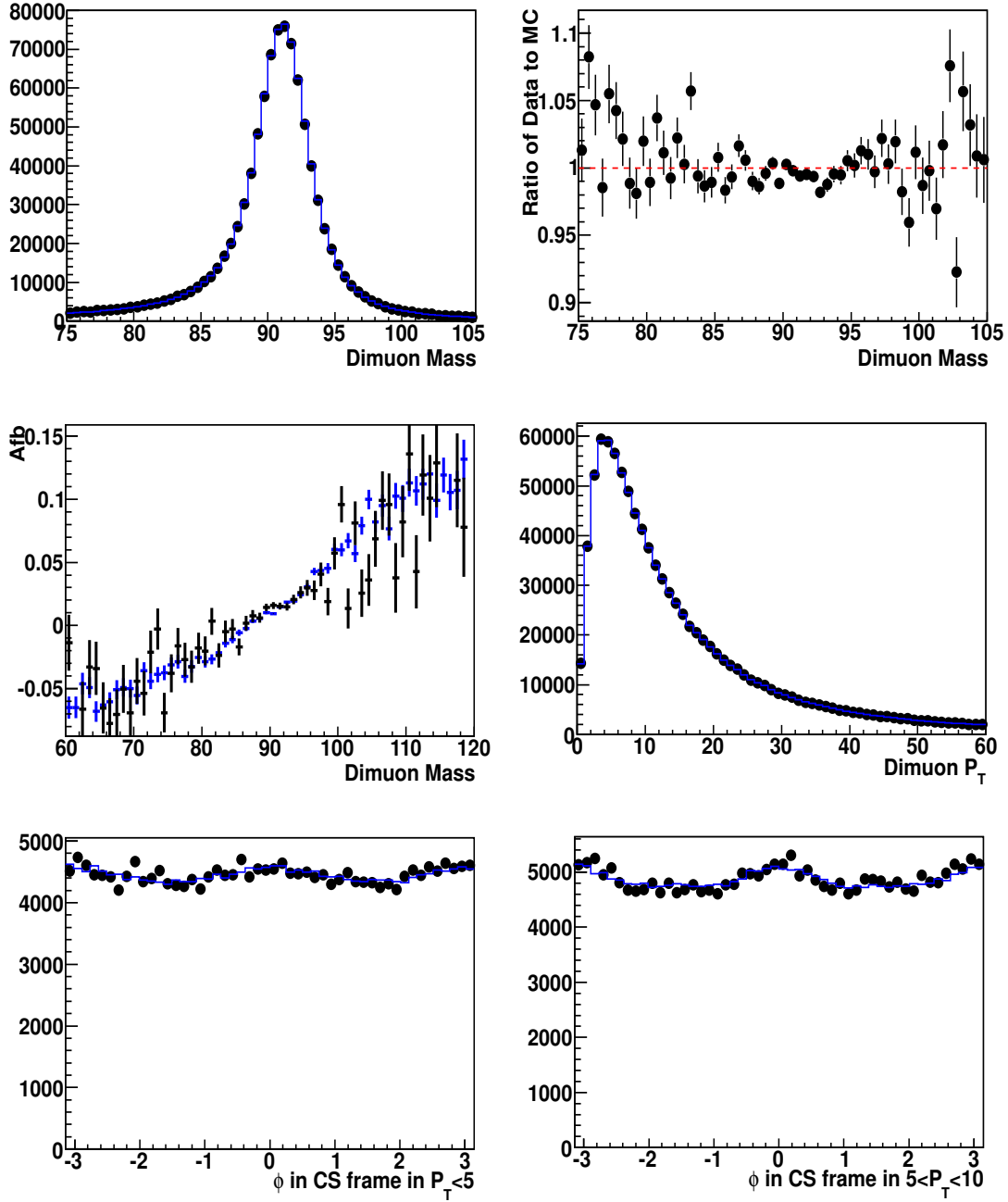


Figure 11: 2011A (2 fb^{-1}) data Iteration 1: The reference plots ($M_{\mu^+\mu^-}$, A_{fb} , $Z P_T$, and ϕ_{CS}) after the iteration 1 muon momentum correction and $Z P_T$ correction. Top Plots: Comparison of the dimuon invariant mass distribution between the data (black) and MC (blue) (left) and its ratio of data to MC (right). Middle plots: Comparison of A_{fb} (left) and boson P_T (right) distributions between the data (black) and MC (blue). Bottom plots: Comparison of ϕ in the Collins-Soper frame in boson $P_T < 5 \text{ GeV}/c$ (left) and ϕ in the Collins-Soper frame in boson $5 < P_T < 10 \text{ GeV}/c$ (right) distributions between the data (black) and MC (blue). The plots are normalized to the total number of events of the data in $60 < M_{\mu\mu} < 120 \text{ GeV}/c^2$.

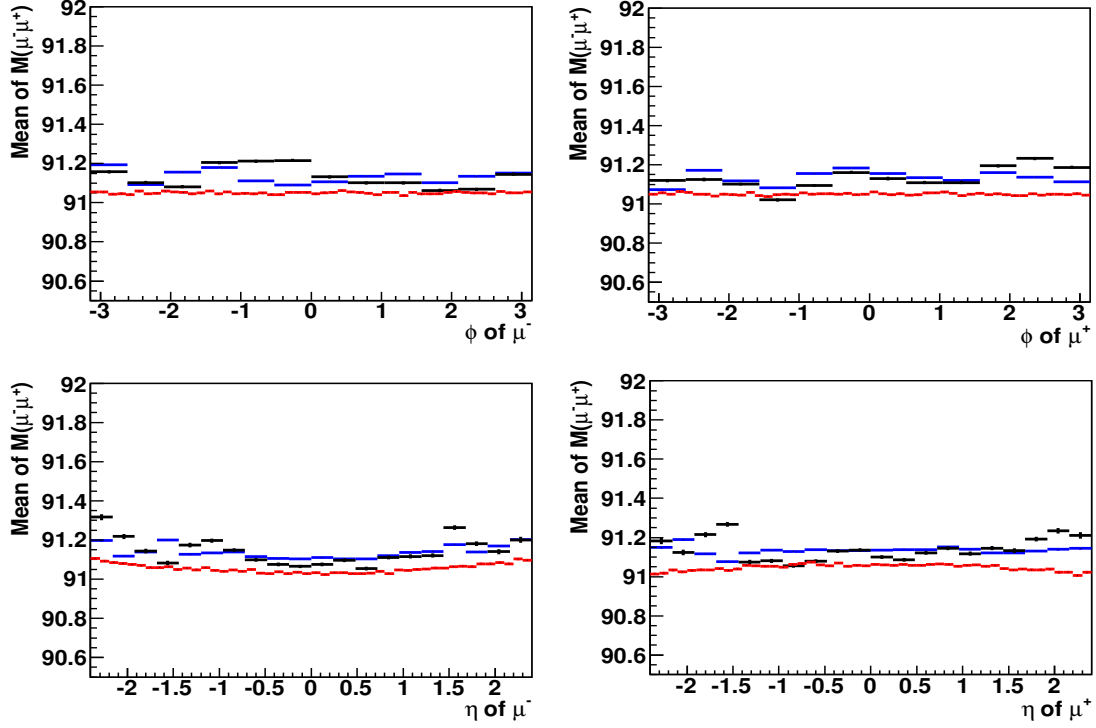


Figure 12: The $M_{\mu^+\mu^-}$ profile plot as a function of η and ϕ of μ^+ and μ^- after applying the iteration 1 muon momentum correction and Z P_T correction. Top Plots: Comparison of the average of $M_{\mu\mu}$ in ϕ of μ^- (left) and the average of $M_{\mu\mu}$ in ϕ of μ^+ (right) between the data (black) and MC (blue). Bottom Plots: Comparison of the average of $M_{\mu\mu}$ in η of μ^- (left) and the average of $M_{\mu\mu}$ in η of μ^+ (right) between the data (black) and MC (blue). The red points are the $M_{\mu\mu}$ profile plot as a function of ϕ and η for μ^+ and μ^- in the generated level. The peak of $M_{\mu\mu}$ in data and MC is matched to be $M_{\mu\mu}$ of the generated level after the kinematic selections ($P_T > 20 \text{ GeV}$ and $|\eta| < 2.4$ for both muons), but the mean of $M_{\mu\mu}$ in the generated level is smaller than the reconstructed level because of the smearing effect. The average of Z mass is obtained from the tight mass window, $86.5 < M_{\mu\mu} < 96.5 \text{ GeV}/c^2$.

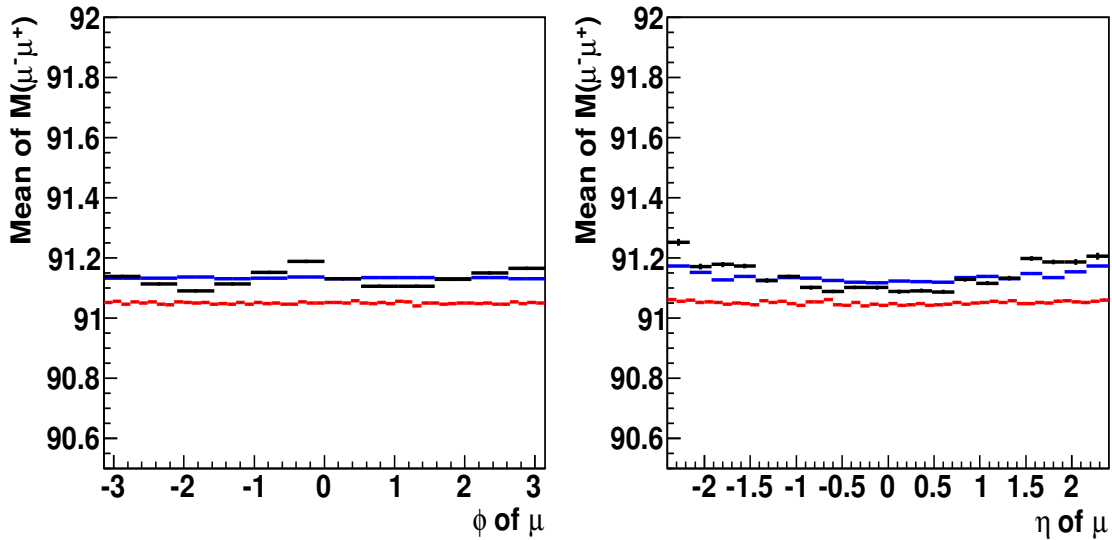


Figure 13: The $M_{\mu^+\mu^-}$ profile plot as a function of ϕ (left) and η (right) of μ (no charge requirement) after applying the iteration 1 muon momentum additive correction and Z P_T correction. The average of Z mass is obtained from the tight mass window, $86.5 < M_{\mu\mu} < 96.5 \text{ GeV}/c^2$.

8 Appendix

8.1 Test of Momentum in High Mass Region

We study the muon momentum scale using the events in Z mass region, $60 < M_{\mu^+\mu^-} < 120 \text{ GeV}/c^2$. The muon momentum scale is used for not only in the Zmass region, but also in the high mass region (where muons a very high P_T). Therefore, we test how the momentum scale corrections perform in the high momentum region. Since we know the true momentum in the MC, we can compare the true momentum to the reconstructed MC momentum (after our scale and alignment correction).

To select the high momentum muons, we select the events at high mass, $M_{\mu^+\mu^-} > 250 \text{ GeV}/c^2$ and compare the average of $1/p_T$, $\langle 1/p_T \rangle$, in the MC reconstructed level to the average of $1/p_T$ in the generated (smeared) level as a function of charge, η , and ϕ . Here, it is the generated momentum post FSR without resolution smearing.

The difference of $\langle 1/p_T \rangle$ between the reconstructed and the generated level (smeared) is close to be zero within 1 standard deviation for all charge, η , and ϕ bins. Figure 23 shows the difference of $\langle 1/p_T \rangle$ between the reconstructed and the generated level (smeared) in the Z mass region ($60 < M_{\mu^+\mu^-} < 120 \text{ GeV}/c^2$), and in the high mass, $M_{\mu^+\mu^-} > 250 \text{ GeV}/c^2$ region.

8.2 Test of the MuscleFit Correction

In this appendix, we show that the MuscleFit correction does not fully correct for the momentum scale and misalignments in either data or MC.

The MuscleFit correction was the standard method to correct the muon momentum bias in 2010. The MuscleFit is available for the first 750 pb^{-1} of the 2011A data[1]. It is not available for the rest of the 2011A (2 fb^{-1}) data sample..

No MuscleFit is available for any part of the 2011A (2.1 fb^{-1}) Monte Carlo samples. MuscleFits for MC are only available for the 2010 MC samples.

In our study, we first apply the MuscleFit extracted from first 750 pb^{-1} of the 2011A data set to the all of the 2011A (2.1 fb^{-1}) data set. Since no MuscleFit is available for any of the 2011 MC samples, we try to see what happens if we apply MuscleFit for the 2010 MC to the 2011A MC.

To test the performance of the MuscleFit, we use the reference plots which are described in Sec. 3. Figure 24 and 25 show the reference plots for the data (2011A 2.1 fb^{-1}) and Figure 26 and 27 show the reference plots for 2011 MC. For all of these plots we show the reference variables before (black) and after (blue) applying the MuscleFit

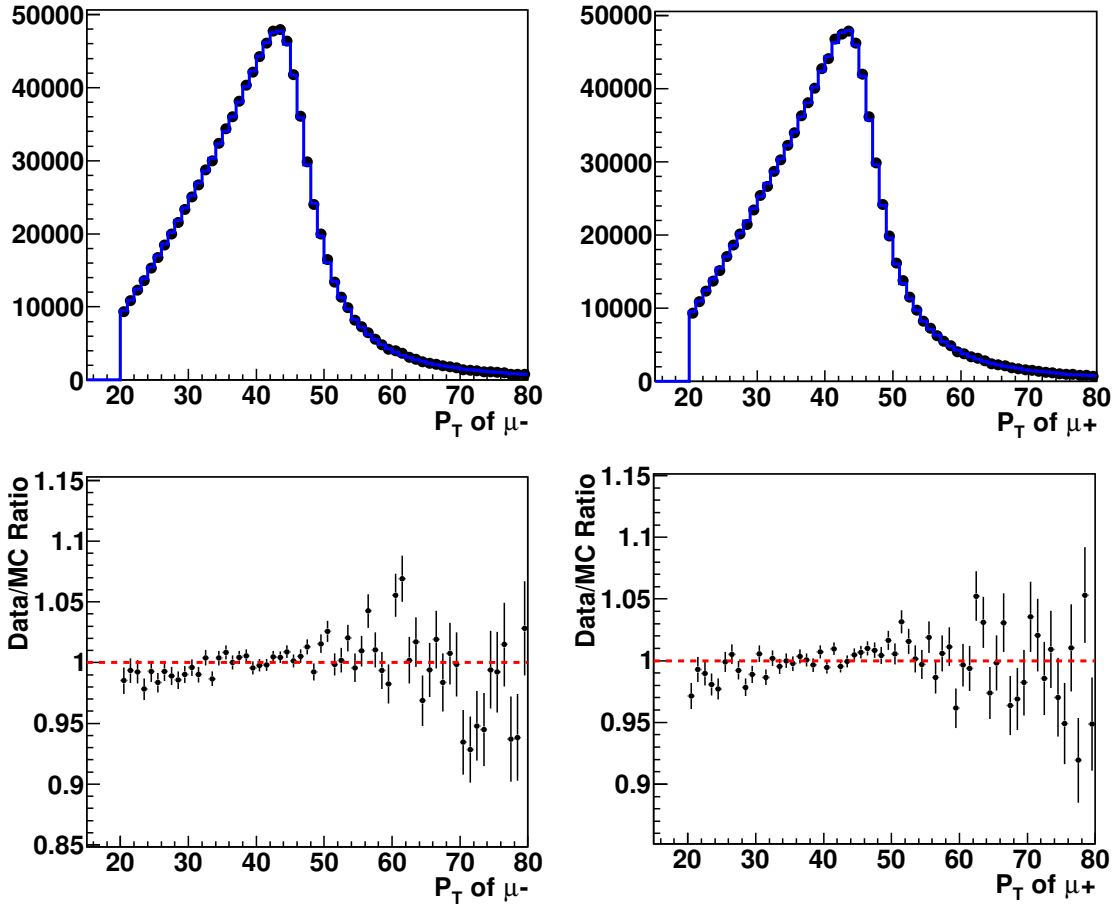


Figure 14: 2011A (2 fb⁻¹) Iteration 1: The muon p_T spectrum in the data and MC and its ratio after applying iteration 1 muon momentum correction and Z P_T correction. Top Plots: Comparison of the p_T distribution between the data (black) and MC (blue) for μ^- (left) and μ^+ (right) after applying iteration 1 muon additive momentum correction and Z P_T correction. Bottom plots: The ratio of muon p_T distribution for μ^- (left) and μ^+ (right) The plots are normalized to the total number of events of the data in $60 < M_{\mu\mu} < 120 \text{ GeV}/c^2$.

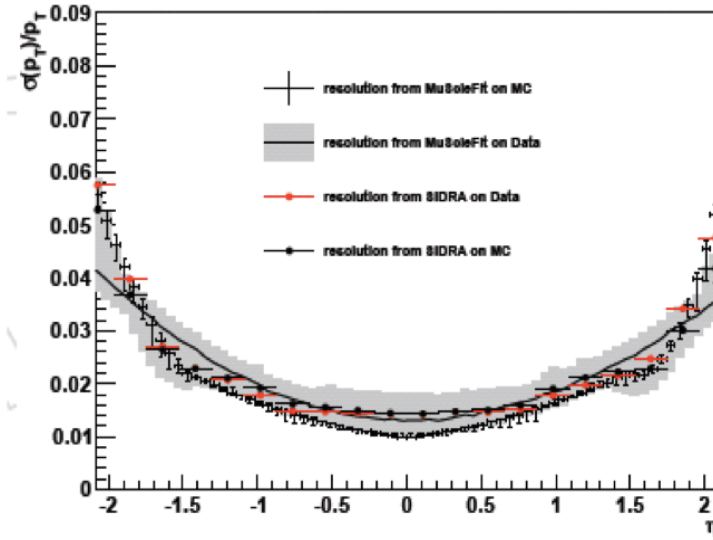


Figure 15: The resolution of muon momentum as a function of muon η . The η dependent resolution smearing is applied to generated muon momentum. This plot was obtained from SIDRA

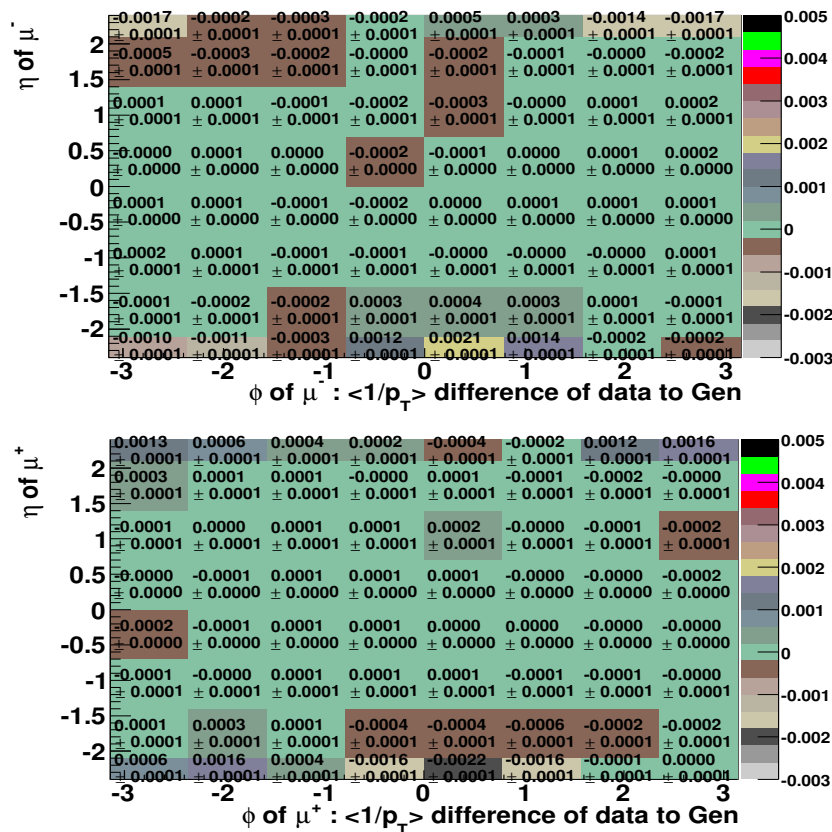


Figure 16: (2011A (2 fb⁻¹) iteration 2 : The $\langle 1/p_T \rangle$ correction for data for μ^- (top) and μ^+ (bottom) in η and ϕ .

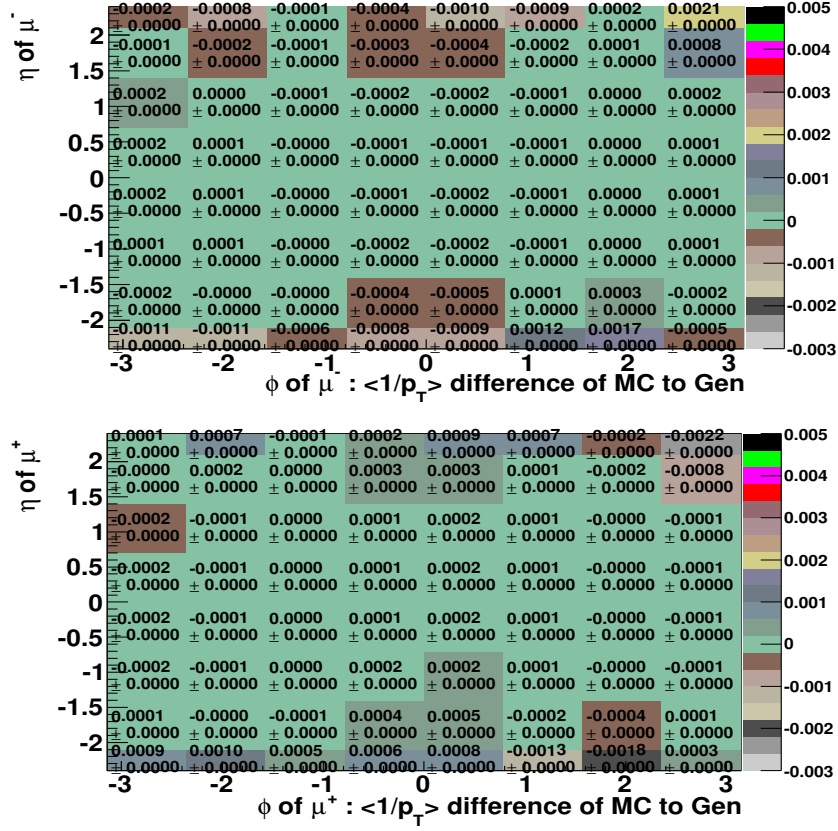


Figure 17: (2011A (2 fb⁻¹) iteration 2 : The $\langle 1/p_T \rangle$ correction for MC for μ^- (top) and μ^+ (bottom) in η and ϕ .

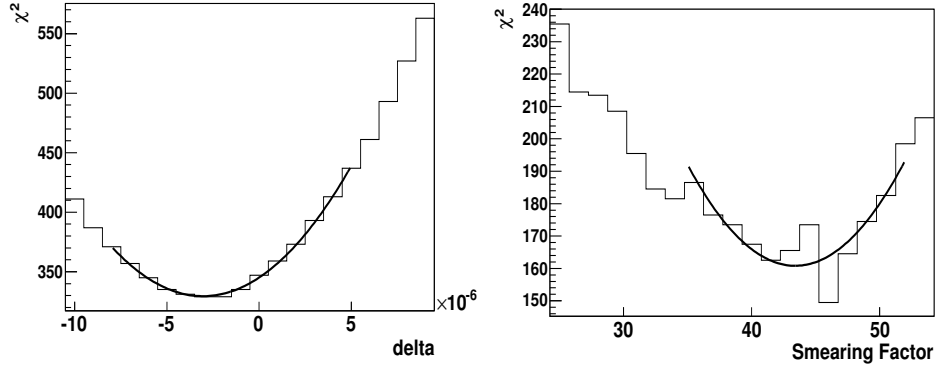


Figure 18: (2011A (2 fb⁻¹) iteration 2 : χ^2 distribution as a function of the global factor, Δ (left) and SF (right).

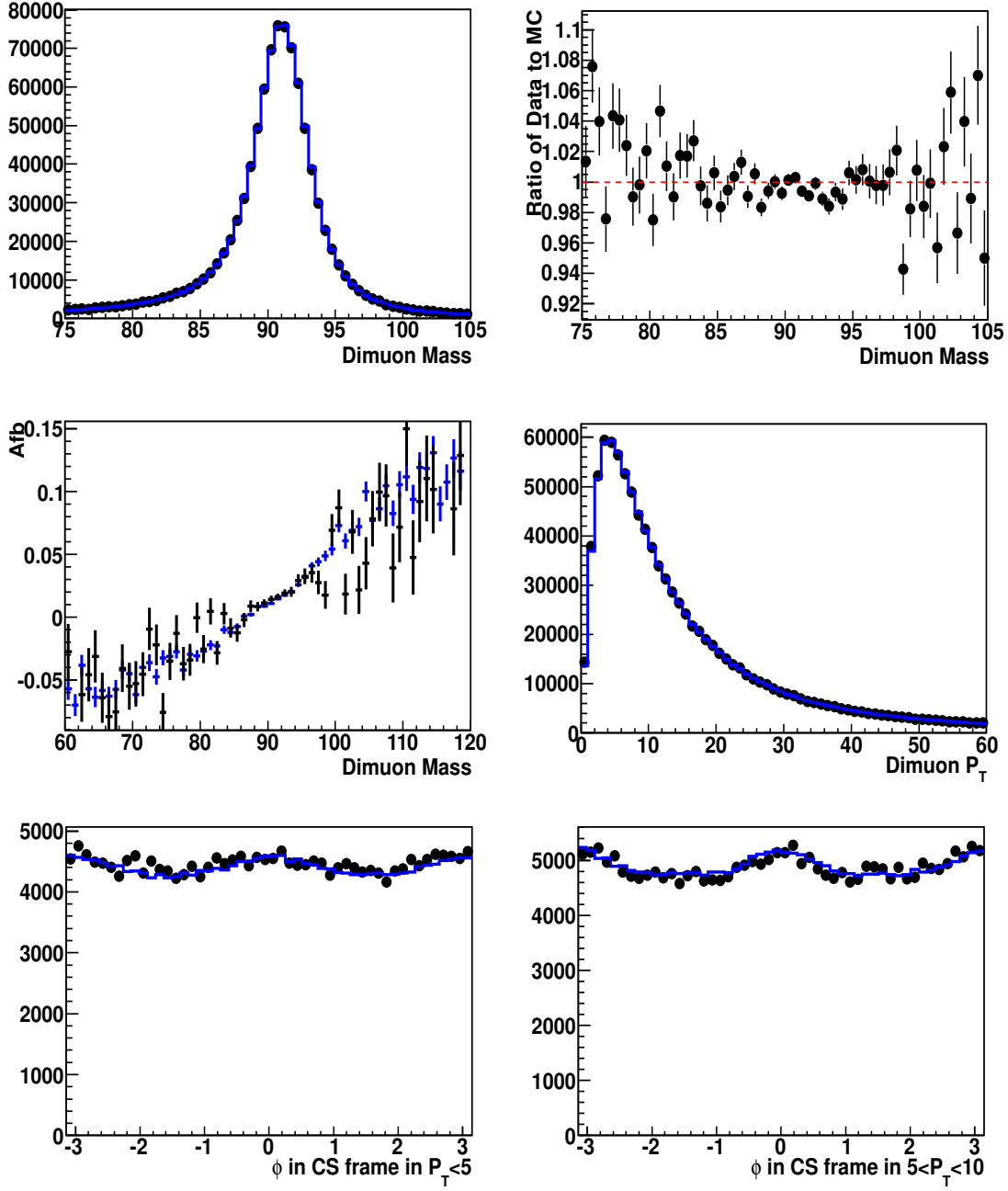


Figure 19: 2011A (2 fb⁻¹) iteration 2 : The reference plots ($M_{\mu^+\mu^-}$, A_{fb} , $Z P_T$, and ϕ_{CS}) after the application of the iteration 2 muon momentum correction. Top Plots: Comparison of the dimuon invariant mass distribution between the data (black) and MC (blue) (left) and its ratio of data to MC (right). Middle plots: Comparison of A_{fb} (left) and boson P_T (right) distributions between the data (black) and MC (blue). Bottom plots: Comparison of ϕ in the Collins-Soper frame in boson $P_T < 5 \text{ GeV}/c$ (left) and ϕ in the Collins-Soper frame in boson $5 < P_T < 10 \text{ GeV}/c$ (right) distributions between the data (black) and MC (blue). The plots are normalized to the total number of events of the data in $60 < M_{\mu\mu} < 120 \text{ GeV}/c^2$.

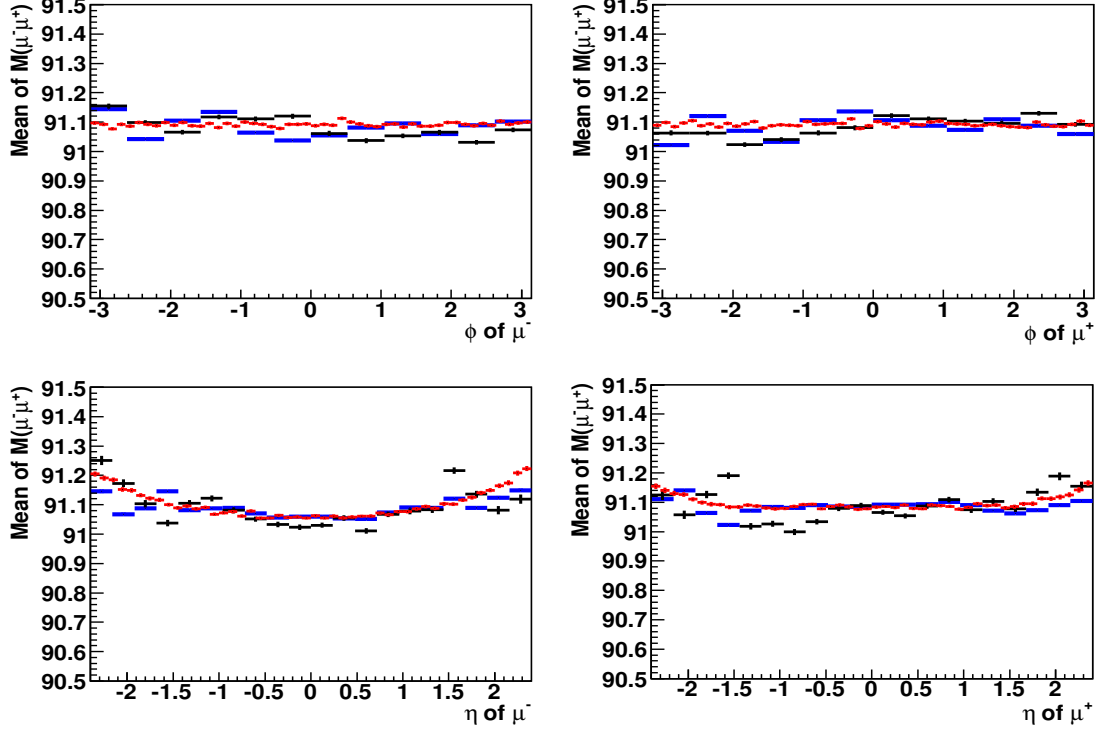


Figure 20: 2011A (2 fb⁻¹) iteration 2: The $M_{\mu^+\mu^-}$ profile plot as a function of η and ϕ of μ^+ and μ^- after the iteration 2 muon momentum correction. Top Plots: Comparison of the average of $M_{\mu\mu}$ in ϕ of μ^- (left) and the average of $M_{\mu\mu}$ in ϕ of μ^+ (right) between the data (black) and MC (blue). Bottom Plots: Comparison of the average of $M_{\mu\mu}$ in η of μ^- (left) and the average of $M_{\mu\mu}$ in η of μ^+ (right) between the data (black) and MC (blue). The red points are the $M_{\mu\mu}$ profile plot as a function of ϕ and η for μ^+ and μ^- in the generated level. The average of $M_{\mu\mu}$ is obtained in the Z peak region, $86.5 < M_{\mu\mu} < 96.5$ GeV/ c^2 .

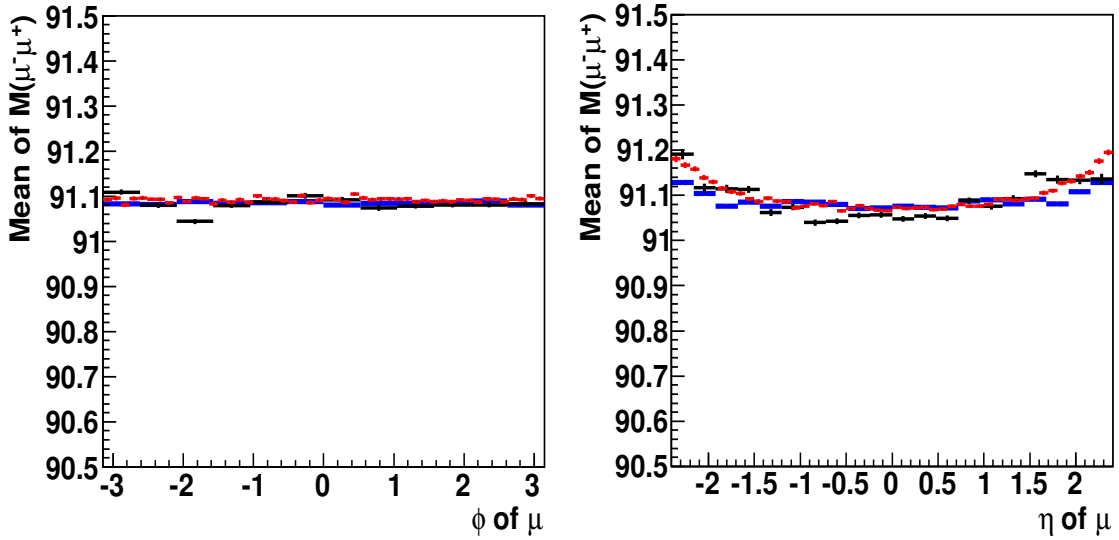


Figure 21: 2011A (2 fb⁻¹) iteration 2. The $M_{\mu^+\mu^-}$ profile plot as a function of ϕ (left) and η (right) of μ (no charge requirement) after applying the iteration 2 muon momentum correction. The average of $M_{\mu\mu}$ is obtained in the Z peak region, $86.5 < M_{\mu\mu} < 96.5$ GeV/ c^2 .

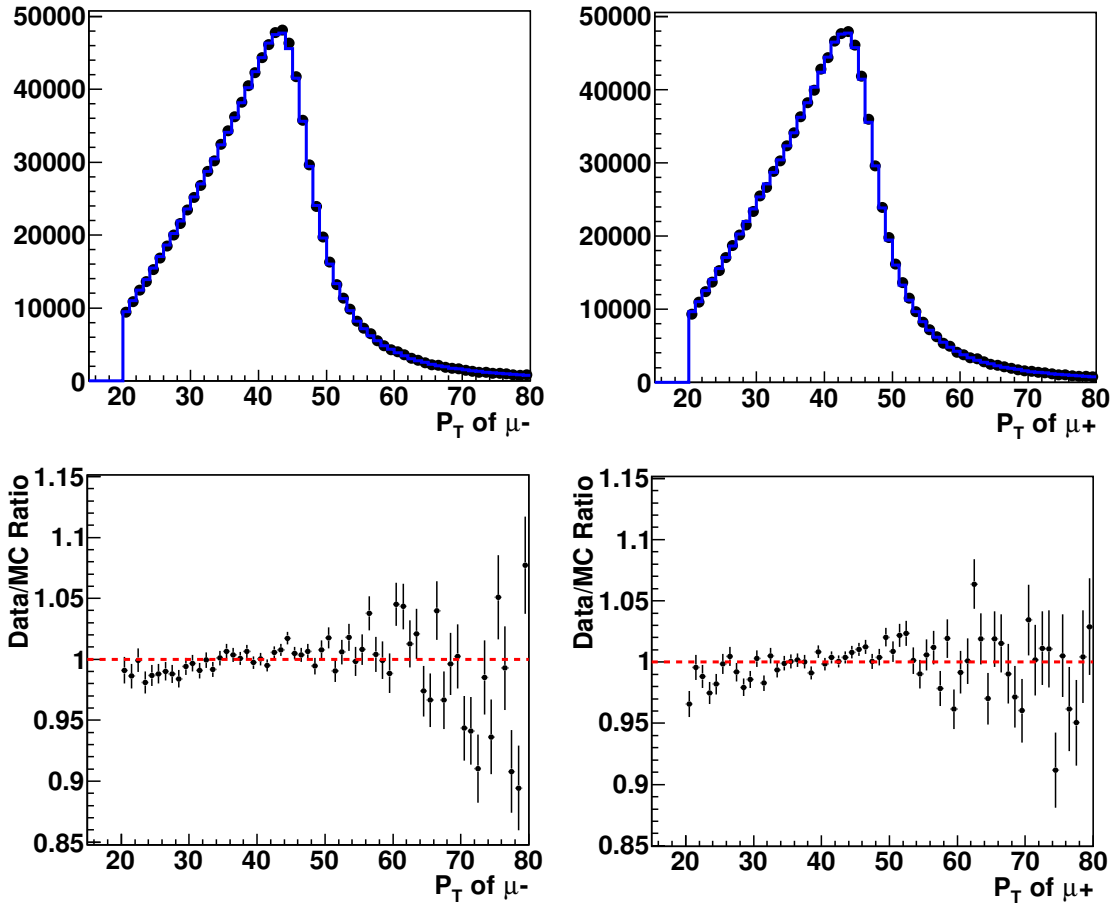


Figure 22: 2011A (2 fb^{-1}). The muon p_T spectrum in the data and MC and its ratio after the iteration 2 muon momentum correction and Z P_T correction. Top Plots: Comparison of the p_T distribution between the data (black) and MC (blue) for μ^- (left) and μ^+ (right) after the iteration 1 muon additive momentum correction and Z P_T correction. Bottom plots: The ratio of muon p_T distribution for μ^- (left) and μ^+ (right) The plots are normalized to the total number of events of the data in $60 < M_{\mu\mu} < 120 \text{ GeV}/c^2$.

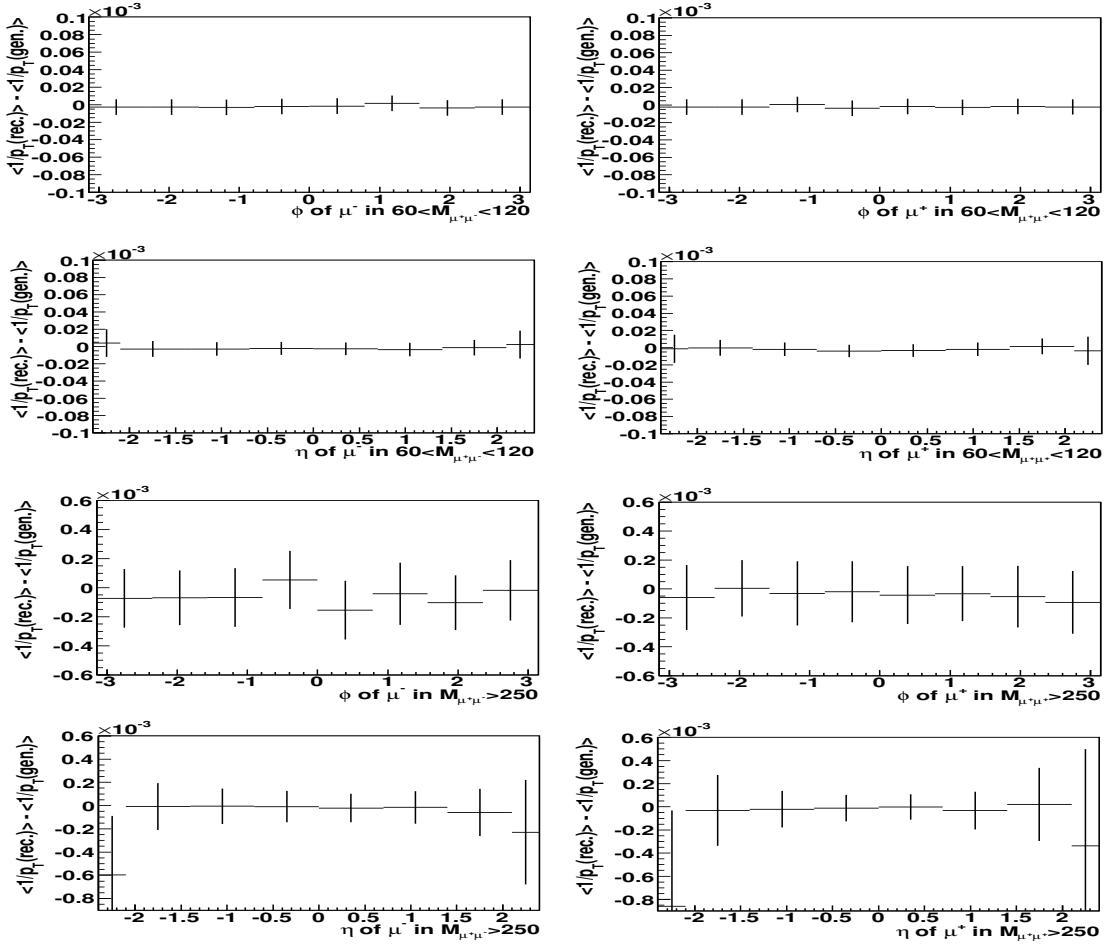


Figure 23: 2011A (2 fb⁻¹) iteration 2. MC test of the muon momentum correction at Z mass and the high mass: The difference of $\langle 1/p_T(\text{rec.}) \rangle$ and $\langle 1/p_T(\text{gen.}) \rangle$ (*smeared*) in $60 < M_{\mu^+\mu^-} < 120 \text{ GeV}/c^2$ and $M_{\mu^+\mu^-} > 250 \text{ GeV}/c^2$. Top plot: The difference of $\langle 1/p_T(\text{rec.}) \rangle$ and $\langle 1/p_T(\text{gen.}) \rangle$ (*smeared*) after applying the muon momentum correction (iteration 2) for μ^- (left) and μ^+ (right) in Z mass region, $60 < M_{\mu^+\mu^-} < 120 \text{ GeV}/c^2$. Bottom plot: The difference of $\langle 1/p_T(\text{rec.}) \rangle$ and $\langle 1/p_T(\text{gen.}) \rangle$ (*smeared*) after applying the muon momentum correction (iteration 2) for μ^- (left) and μ^+ (right) in the high mass region, $M_{\mu^+\mu^-} > 250 \text{ GeV}/c^2$.

315 corrections. Both data and MC use are for $|\eta| < 2.4$ (Note that the MuscleFit was only extracted with $|\eta| < 2.1$).
316 After applying the MuscleFit for the data and MC, both data and MC still have a ϕ and η dependence of the muon
317 momentum. In addition, there are wiggles around Z peak region in A_{fb} . Therefore, these cannot be used to fully
318 correct the 2.1 fb^{-1} 2011A sample.

319 Next, we test the MuscleFit and SIDRA corrections only on the data set and η range for which they are supposed
320 to be valid i.e. for the first 750 pb^{-1} and only for $|\eta| < 2.1$ (that sample was used to extract the MuscleFit and
321 SIDRA corrections). Figure 28 and 29 show the reference plots for the MuscleFit and Figure 30 and 31 show the
322 reference plots for SIDRA for 750 pb^{-1} data for the restricted region $|\eta| < 2.1$. Here, the MuscleFit and SIDRA
323 reduce the ϕ dependence of the muon momentum. The η dependence is not corrected for and the wiggles in A_{fb}
324 remains, thus indicating that there is a bias between positive and negative muons. This bias between positive and
325 negative muons is also seen in the $\phi(\text{CS})$ plots (the peaks at $\phi(\text{CS})=0$ and $\phi(\text{CS})=\pm\pi$ are not equal).

326 Next, for the same 750 pb^{-1} data set, we test both corrections up to $|\eta| < 2.4$ as shown in Figure 32 and Figure
327 33 for the MuscleFit, and Figure 34 and Figure 35 for SIDRA, respectively. The $2.1 < |\eta| < 2.4$ region has a
328 different ϕ and η dependence from the lower η region. The MuscleFit and SIDRA correction do not remove the ϕ
329 dependence for $2.1 < |\eta| < 2.4$. The wiggles in A_{FB} are now larger indicating a larger bias between positive and
330 negative muon momentum.

331 In summary, with both MuscleFit or SIDRA correction we still see unphysical wiggles in A_{fb} (in both data and
332 MC) which indicate mis-calibration between positive and negative muons in both samples. The fact that the peaks
333 in the $\phi(\text{CS})=0$ and $\pm\pi$ are not equal in height also indicates that there is a mis-calibration between positive and
334 negative muons in the data which is not corrected by MuscleFit or SIDRA.

335 The 2010 MC (2010 November version) has the different alignment scenario than the 2011A MC (2011 Spring
336 version). Therefore, the MuscleFit for the 2010 November version of MC might not work for 2011 Spring version
337 of the MC. We find that this is indeed the case.

338 To compare our corrections (Rochester correction) with MuscleFit and SIDRA, we also show the reference plots
339 before and after Rochester correction for both data and MC. Figure 36 and 36 show the reference plots before
340 (black) and after (blue) for the 2011A data and Figure 38 and 38 show the reference plots for the MC. The Rochester
341 correction fully corrects the data as well as the MC for the entire 2011A data, and the full range in η up to $\eta = 2.4$.

342 **8.3 Incremental Rochester Correction on top of MuscleFit and SIDRA**

343 As described in Sec. 8.2 we find that MuscleFit and SIDRA corrections are not sufficient to remove all eta de-
344 pendence in the muon momentum in the 2011A data. If any of these two corrections are used, one needs to apply
345 further corrections.

346 As a test of our approach we report on the extraction of an incremental rochester correction that can be used on top
347 of the MuscleFit or SIDRA correction when applied to the entire 2011A 2.1 fb^{-1} data sample.

348 For the 2011 MC, no MuscleFit or SIDRA corrections exist. Therefore the only corrections available for the MC
349 are the complete Rochester corrections from iteration 2 which are given in Sec. 5 and shown in 17.

350 Figure 40 and 41 show the $\langle 1/p_T \rangle$ Rochester incremental corrections to be used for the data and applied on top
351 of either MuscleFit or on top of SIDRA, respectively. Table 3 summarizes the global factors for MC to match to
352 the data for which the incremental Rochester correction is applied on top of MuscleFit or SIDRA correction.s

353 Figure 42, 43, and 44 show the reference plots after the application of the incremental Rochester correction of top
354 of the MuscleFit correction. Figure 45, 46, and 47 show the reference plots after the application of the incremental
355 Rochester correction on top the SIDRA correction. After the application of the incremental Rochester correction of
356 top of either MuscleFit or SIDRA corrections, all kinematic distributions and the Z mass profile plots as a function
357 of η and ϕ are greatly improved.

358 **References**

359 [1] MuscleFit for 2011A data set : Presentation in CMS Muon POG Meeting (July. 11th, 2011). The presentation
360 is linked at <https://indico.cern.ch/getFile.py/access?contribId=1&resId=0&materialId=slides&confId=128936>.
361

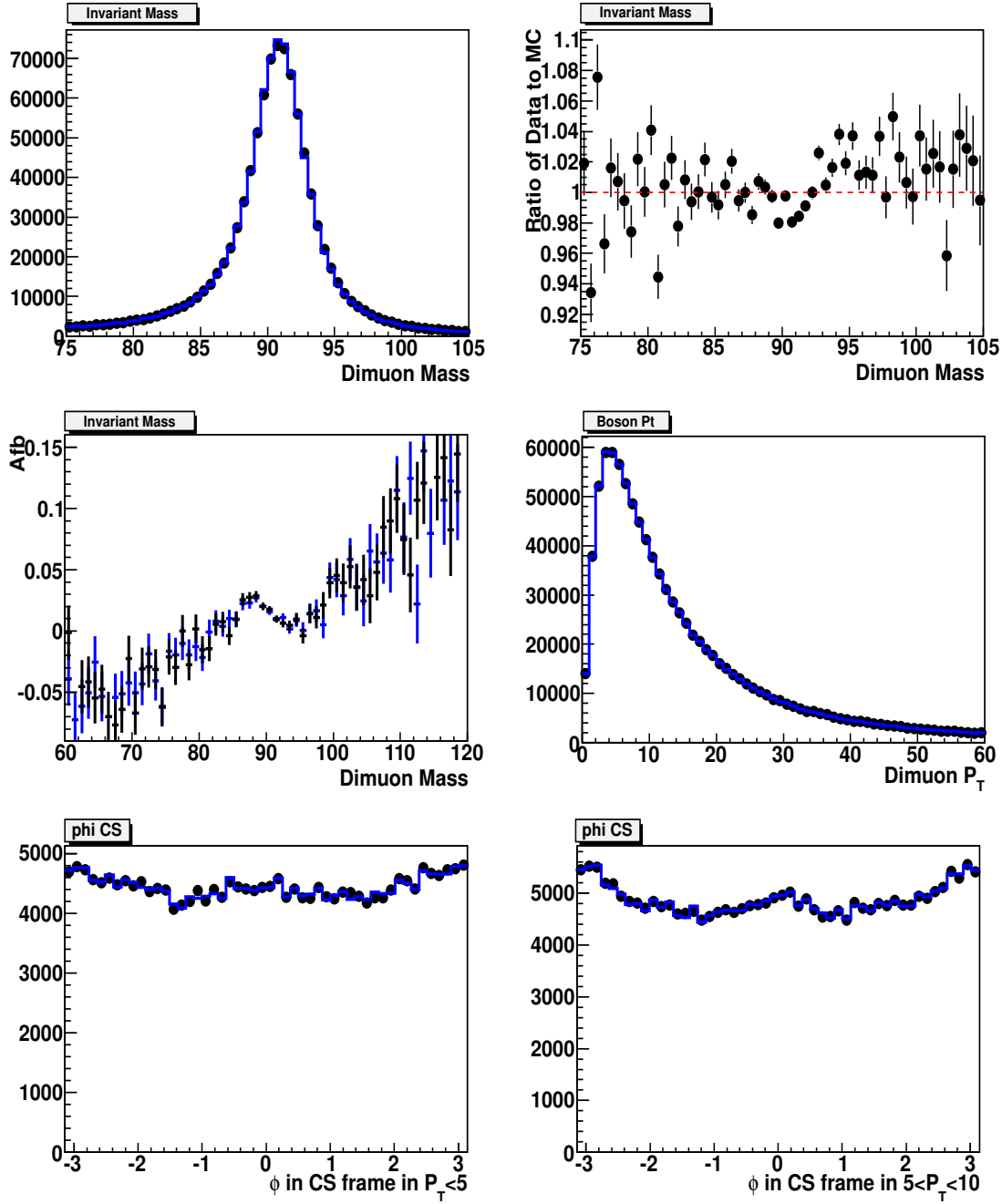


Figure 24: Test of MuscleFit for the 2011A (2 fb^{-1}) data sample: The effect of the MuscleFit correction (for the first 1/3 of the 2011A data) when applied to the full 2011A sample. Top Plots: Comparison of the dimuon invariant mass distribution before (black) and after (blue) applying MuscleFit (left) and its ratio (right). Middle plots: Comparison of A_{fb} (left) and boson P_T (right) distributions before (black) and after (blue) applying MuscleFit correction. Bottom plots: Comparison of ϕ in the Collins-Soper frame in boson $P_T < 5 \text{ GeV}/c$ (left) and ϕ in the Collins-Soper frame in boson $5 < P_T < 10 \text{ GeV}/c$ (right) distributions before (black) after (blue) applying the MuscleFit correction.

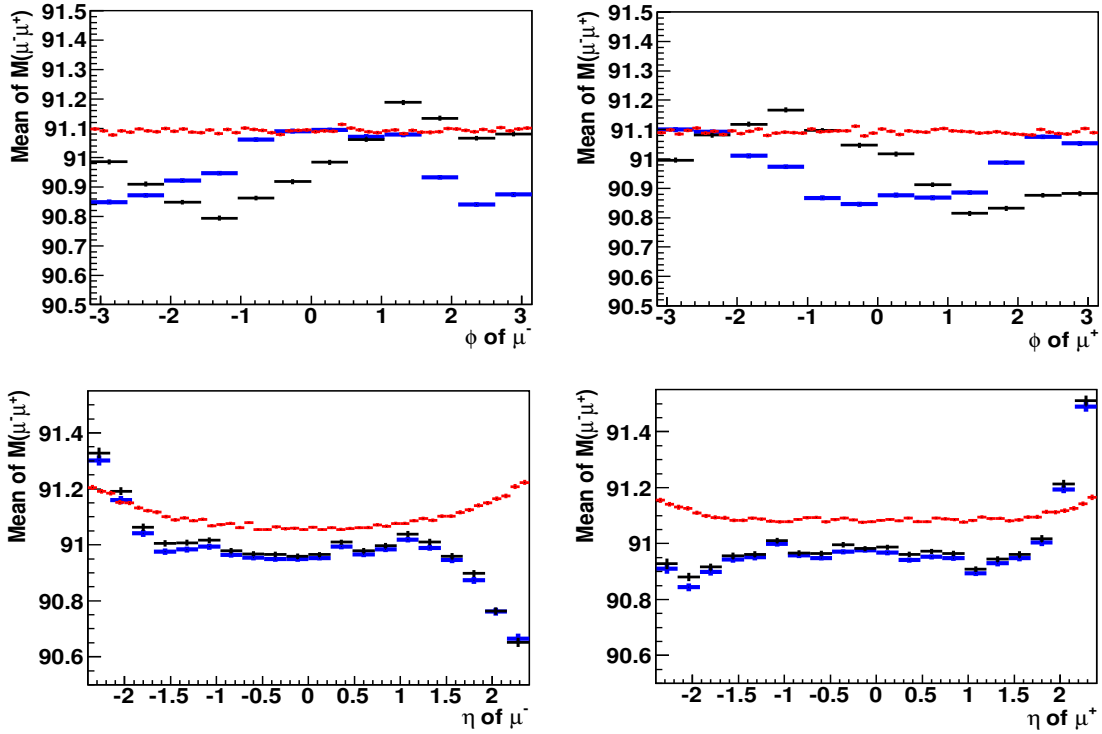


Figure 25: Test of MuscleFit for the 2011A (2 fb^{-1}) data sample: The effect of the MuscleFit correction (for the first 1/3 of the 2011A data) when applied to the full 2011A sample. Top Plots: Comparison of the average of $M_{\mu\mu}$ as a function of ϕ for μ^- (left) and the average of $M_{\mu\mu}$ as function of ϕ for μ^+ (right) before (black) and after (blue) applying the MuscleFit correction. Bottom Plots: Comparison of the average of $M_{\mu\mu}$ as a function of η for μ^- (left) and the average of $M_{\mu\mu}$ as a function of η for μ^+ (right) before (black) and after (blue) applying the MuscleFit correction. The red points are the $M_{\mu\mu}$ profile plot as a function of ϕ and η for μ^+ and μ^- in the generated level. The average of $M_{\mu\mu}$ is obtained in the tight mass window, $86.5 < M_{\mu\mu} < 96.5 \text{ GeV}/c^2$.

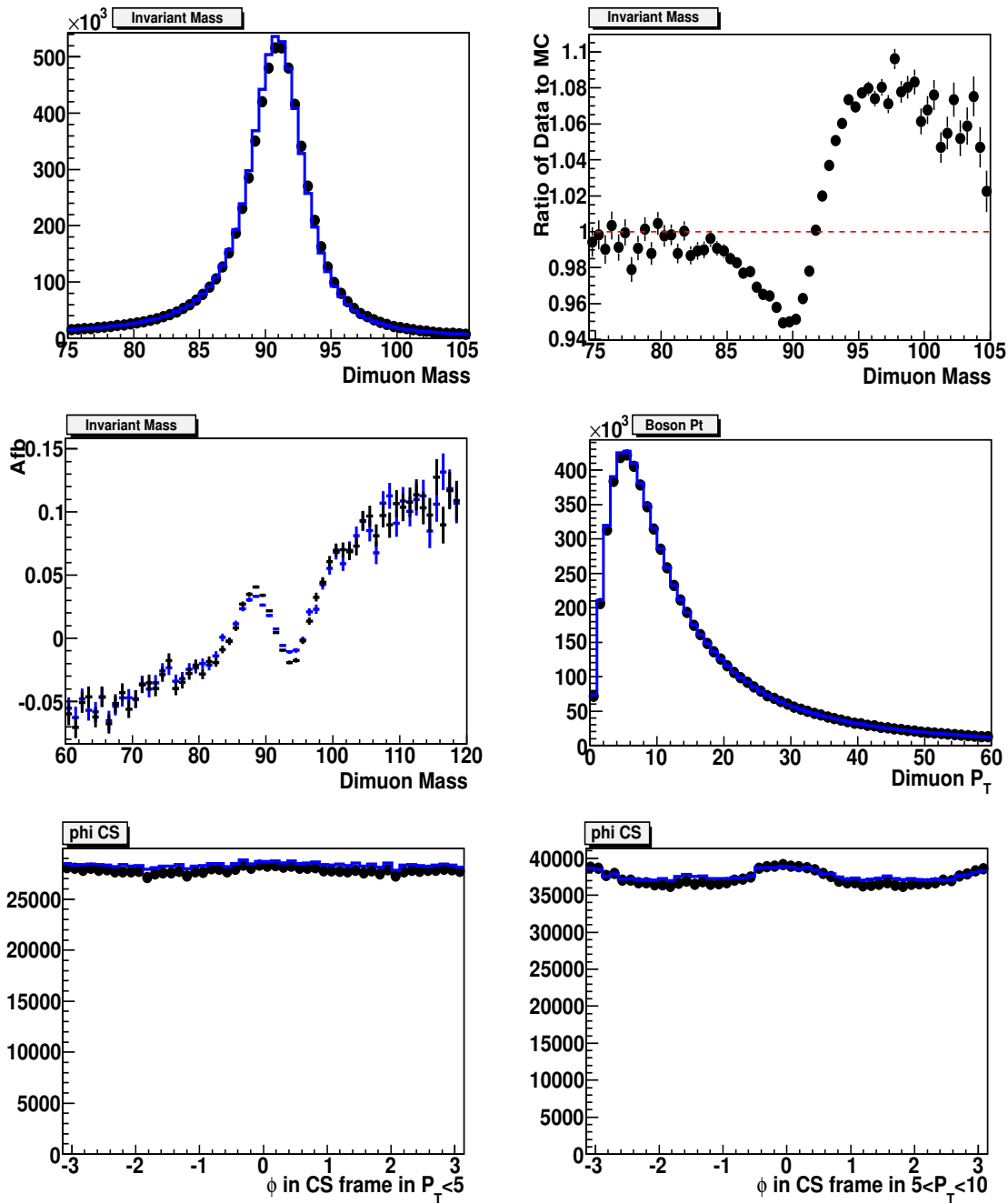


Figure 26: Test of MuscleFi for the 2011A (2 fb^{-1}) MC sample: The effect of using the MuscleFit for the 2010 MC on the 2011A MC sample. Top Plots: Comparison of the dimuon invariant mass distribution before (black) and after (blue) applying MuscleFit (left) and its ratio (right). Middle plots: Comparison of A_{fb} (left) and boson P_T (right) distributions before (black) and after (blue) applying the 2010 MC MuscleFit correction. Bottom plots: Comparison of ϕ in the Collins-Soper frame in boson $P_T < 5 \text{ GeV}/c$ (left) and ϕ in the Collins-Soper frame in boson $5 < P_T < 10 \text{ GeV}/c$ (right) distributions before (black) after (blue) applying the 2010 MC MuscleFit correction.

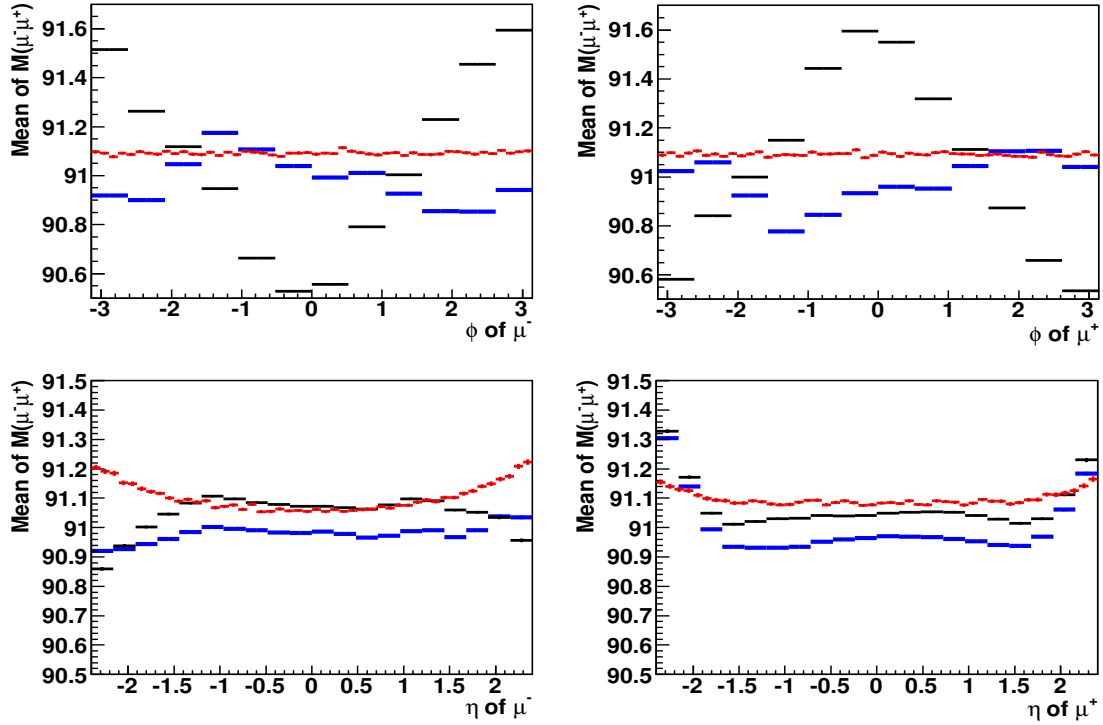


Figure 27: Test of MuscleFit test for the 2011A (2.1 fb^{-1}) MC sample: The effect of using the MuscleFit for the 2010 MC on the 2011A MC sample. Top Plots: Comparison of the average of $M_{\mu\mu}$ as a function of ϕ for μ^- (left) and the average of $M_{\mu\mu}$ as function of ϕ for μ^+ (right) before (black) and after (blue) applying the MuscleFit correction. Bottom Plots: Comparison of the average of $M_{\mu\mu}$ as a function of η for μ^- (left) and the average of $M_{\mu\mu}$ as a function of η for μ^+ (right) before (black) and after (blue) applying the MuscleFit correction. The red points are the $M_{\mu\mu}$ profile plot as a function of ϕ and η for μ^+ and μ^- in the generated level. The average of $M_{\mu\mu}$ is obtained in the tight mass window, $86.5 < M_{\mu\mu} < 96.5 \text{ GeV}/c^2$.

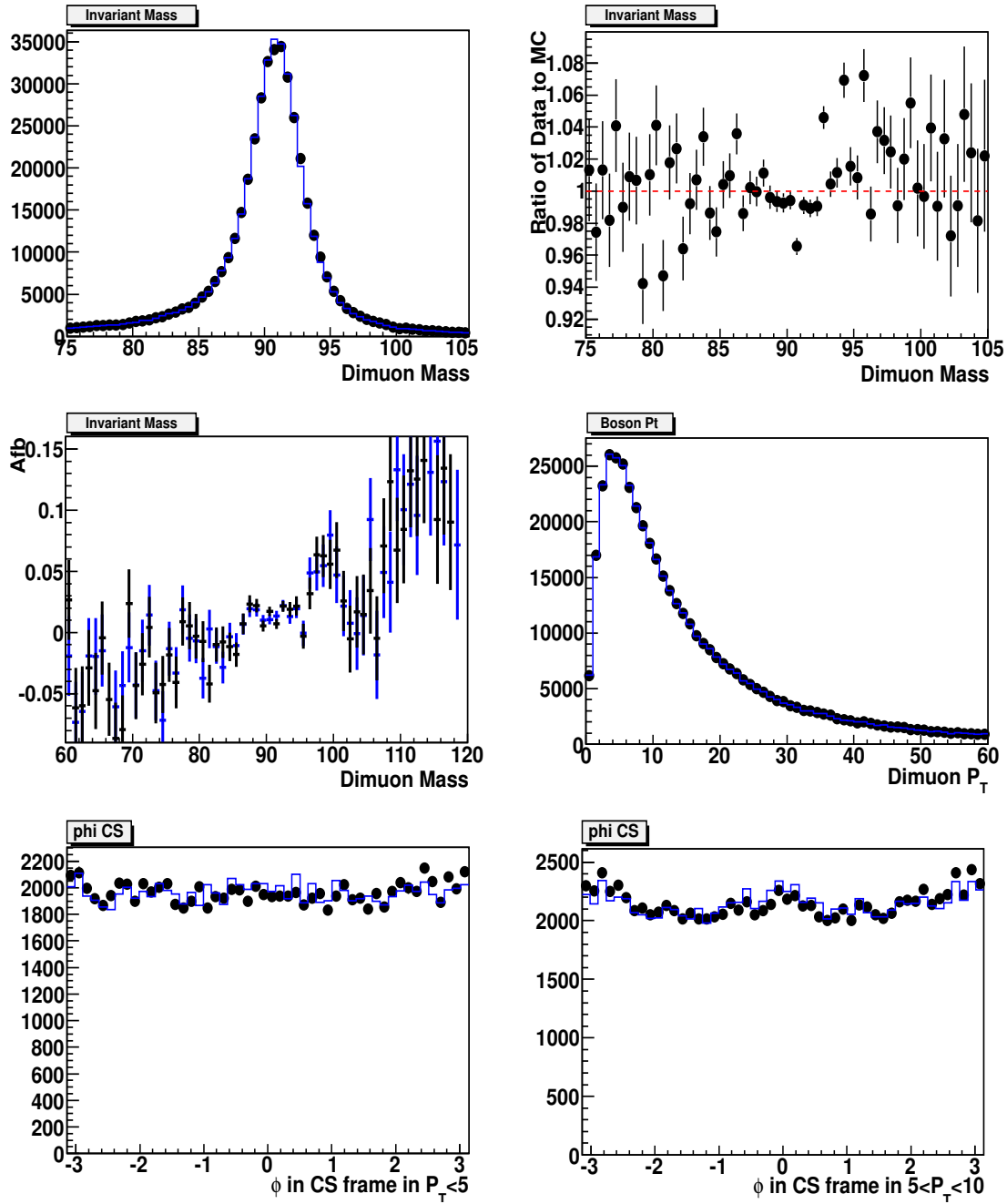


Figure 28: Test of MuscleFit test for the first 750 pb^{-1} and $|\eta| < 2.1$: The effect of the MuscleFit correction (for the first 1/3 of the 2011A data) when applied to the same data set used to determine the parameters of the MuscleFit. Top Plots: Comparison of the dimuon invariant mass distribution before (black) and after (blue) applying MuscleFit (left) and its ratio (right). Middle plots: Comparison of A_{fb} (left) and boson P_T (right) distributions before (black) and after (blue) applying MuscleFit correction. Bottom plots: Comparison of ϕ in the Collins-Soper frame in boson $P_T < 5 \text{ GeV}/c$ (left) and ϕ in the Collins-Soper frame in boson $5 < P_T < 10 \text{ GeV}/c$ (right) distributions before (black) after (blue) applying the MuscleFit correction.

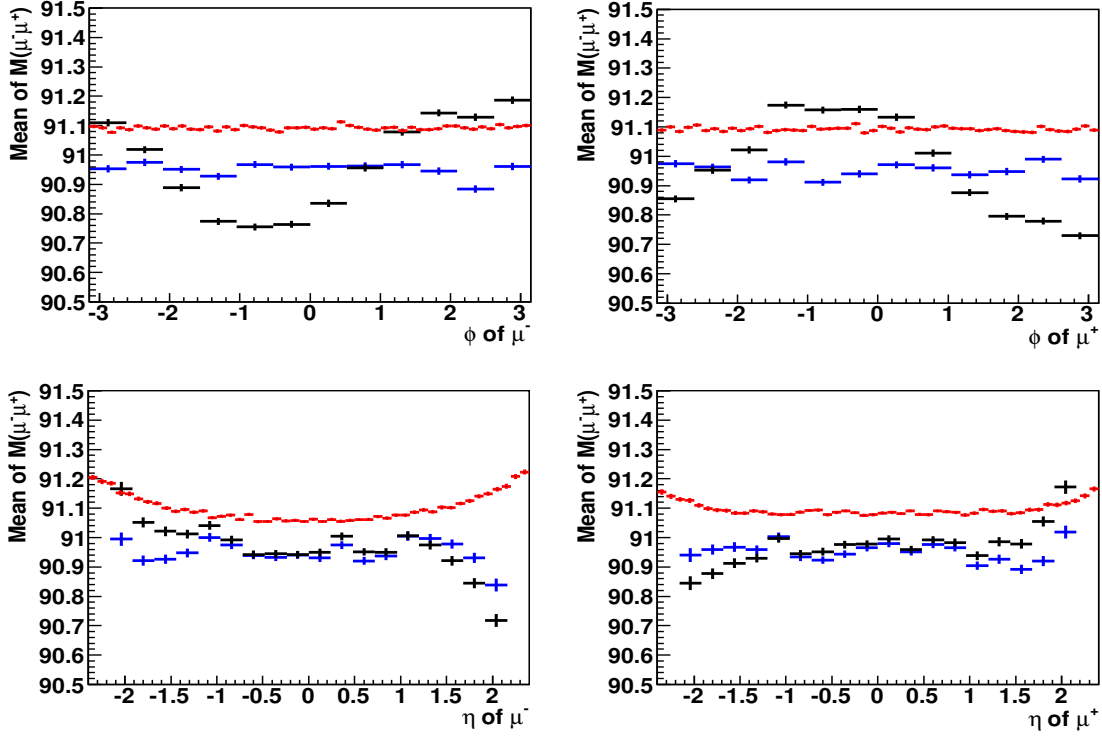


Figure 29: Test of MuscleFit test for the first 750 pb^{-1} and $|\eta| < 2.1$: The effect of the MuscleFit correction (for the first 1/3 of the 2011A data) when applied to the same data set used to determine the parameters of the MuscleFit. Top Plots: Comparison of the average of $M_{\mu\mu}$ as a function of ϕ for μ^- (left) and the average of $M_{\mu\mu}$ as function of ϕ for μ^+ (right) before (black) and after (blue) applying the MuscleFit correction. Bottom Plots: Comparison of the average of $M_{\mu\mu}$ as a function of η for μ^- (left) and the average of $M_{\mu\mu}$ as a function of η for μ^+ (right) before (black) and after (blue) applying the MuscleFit correction. The red points are the $M_{\mu\mu}$ profile plot as a function of ϕ and η for μ^+ and μ^- in the generated level. The average of $M_{\mu\mu}$ is obtained in the tight mass window, $86.5 < M_{\mu\mu} < 96.5 \text{ GeV}/c^2$.

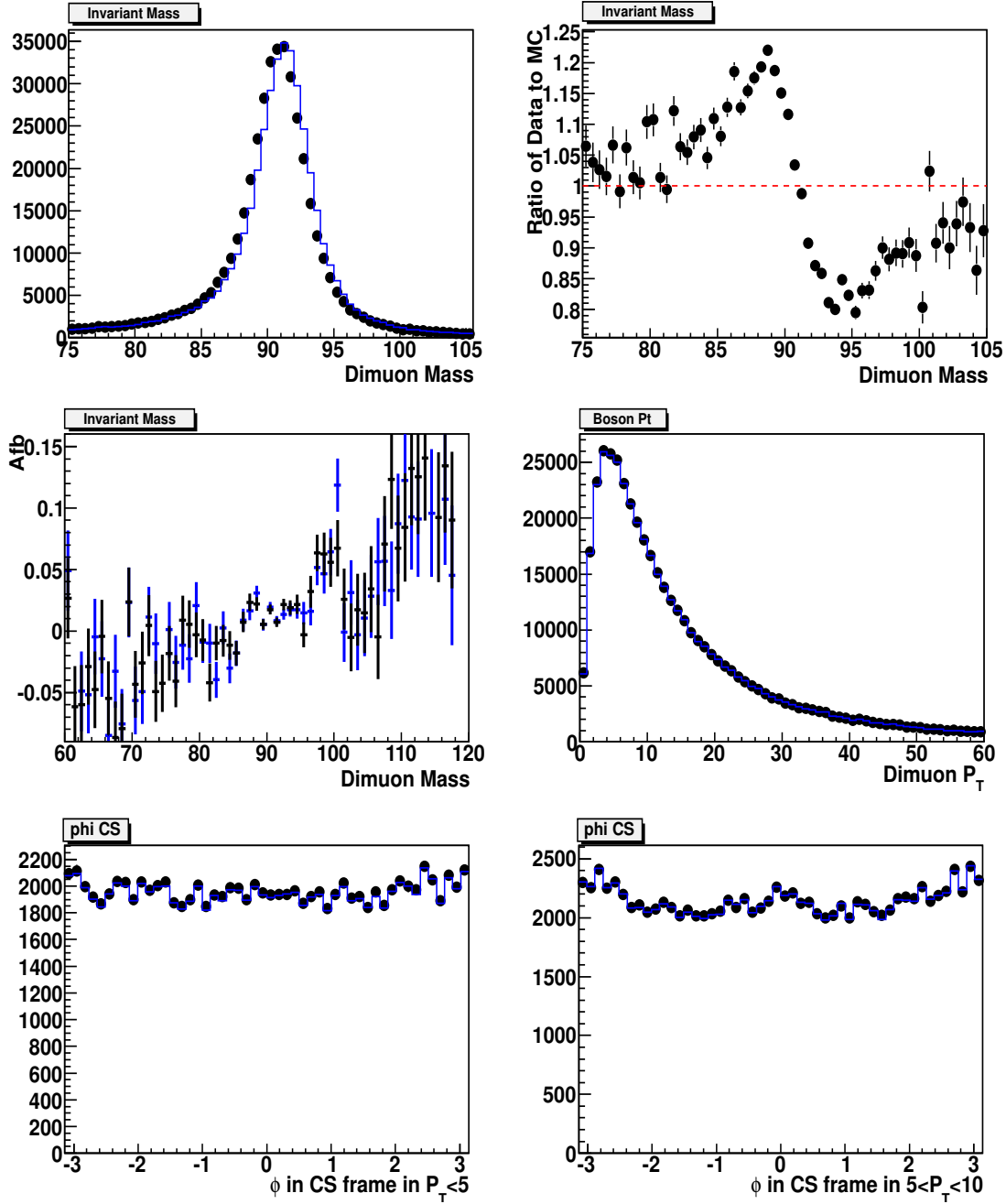


Figure 30: Test of SIDRA for the first 750 pb^{-1} and $|\eta| < 2.1$: The effect of the SIDRA correction (for the first 1/3 of the 2011A data) when applied to the same data set used to determine the parameters of the MuscleFit (similar data set used for SIDRA). Top Plots: Comparison of the dimuon invariant mass distribution before (black) and after (blue) applying SIDRA (left) and its ratio (right). Middle plots: Comparison of A_{fb} (left) and boson P_T (right) distributions before (black) and after (blue) applying SIDRA correction. Bottom plots: Comparison of ϕ in the Collins-Soper frame in boson $P_T < 5 \text{ GeV}/c$ (left) and ϕ in the Collins-Soper frame in boson $5 < P_T < 10 \text{ GeV}/c$ (right) distributions before (black) after (blue) applying the SIDRA correction.

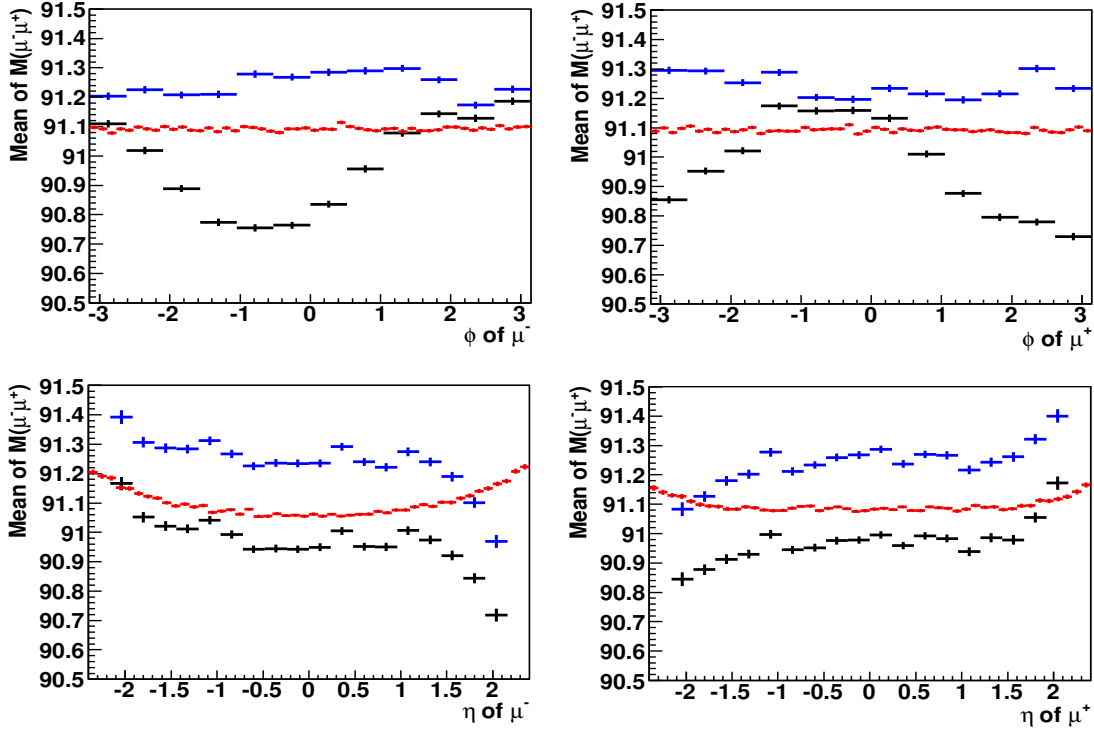


Figure 31: Test of SIDRA for the first 750 pb^{-1} and $|\eta| < 2.1$: The effect of the SIDRA correction (for the first 1/3 of the 2011A data) when applied to the same data set used to determine the parameters of the MuscleFit. (similar data set for used for SIDRA). Top Plots: Comparison of the average of $M_{\mu\mu}$ as a function of ϕ for μ^- (left) and the average of $M_{\mu\mu}$ as function of ϕ for μ^+ (right) before (black) and after (blue) applying the SIDRA correction. Bottom Plots: Comparison of the average of $M_{\mu\mu}$ as a function of η for μ^- (left) and the average of $M_{\mu\mu}$ as a function of η for μ^+ (right) before (black) and after (blue) applying the SIDRA correction. The red points are the $M_{\mu\mu}$ profile plot as a function of ϕ and η for μ^+ and μ^- in the generated level. The average of $M_{\mu\mu}$ is obtained in the tight mass window, $86.5 < M_{\mu\mu} < 96.5 \text{ GeV}/c^2$.

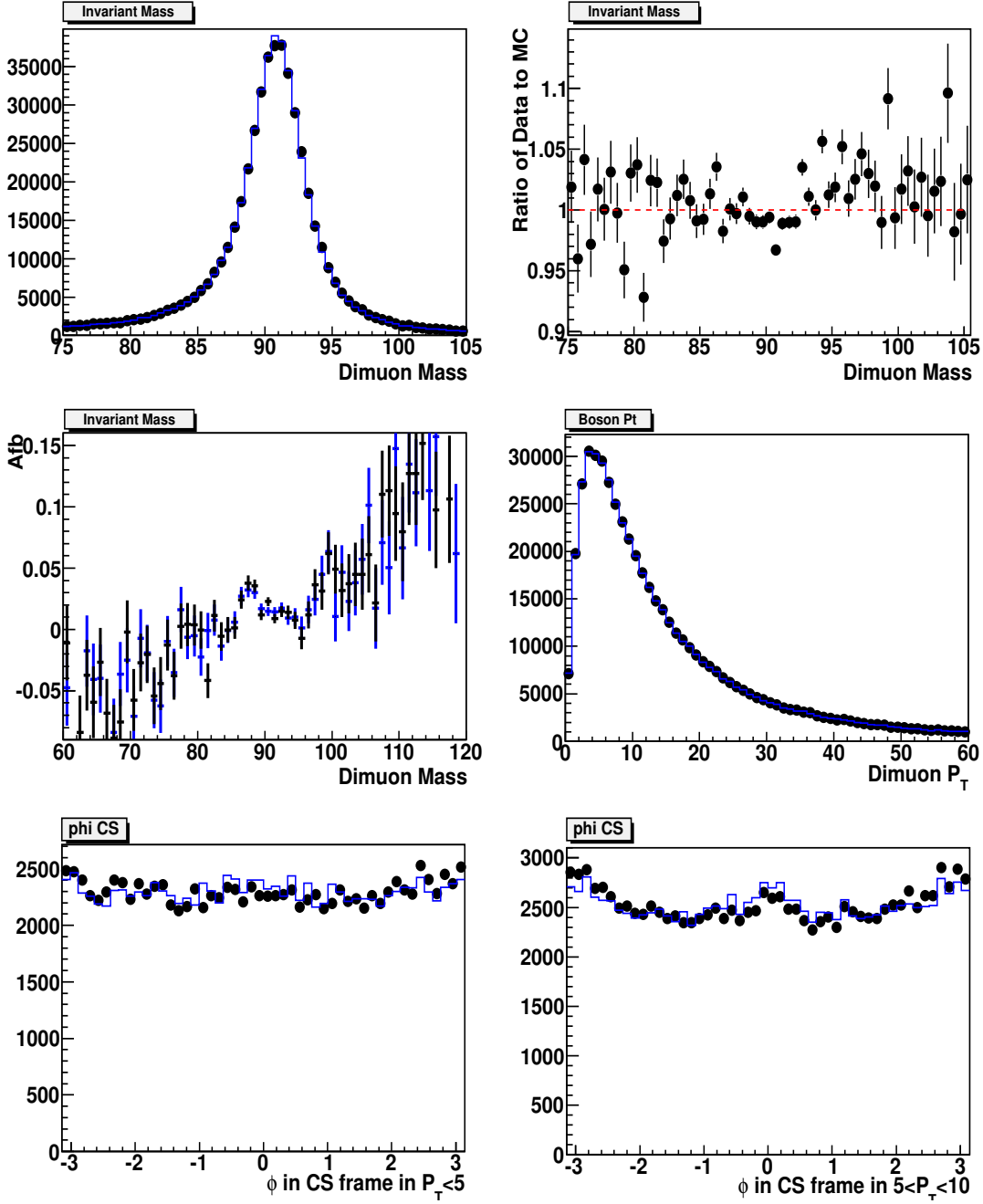


Figure 32: Test of MuscleFit for the first 750 pb^{-1} and $|\eta| < 2.4$: The effect of the MuscleFit correction (for the first 1/3 of the 2011A data) when applied to the same data set used to determine the parameters of the MuscleFit (but only for $|\eta| < 2.1$). Top Plots: Comparison of the dimuon invariant mass distribution before (black) and after (blue) applying MuscleFit (left) and its ratio (right). Middle plots: Comparison of A_{fb} (left) and boson P_T (right) distributions before (black) and after (blue) applying MuscleFit correction. Bottom plots: Comparison of ϕ in the Collins-Soper frame in boson $P_T < 5 \text{ GeV}/c$ (left) and ϕ in the Collins-Soper frame in boson $5 < P_T < 10 \text{ GeV}/c$ (right) distributions before (black) after (blue) applying the MuscleFit correction.

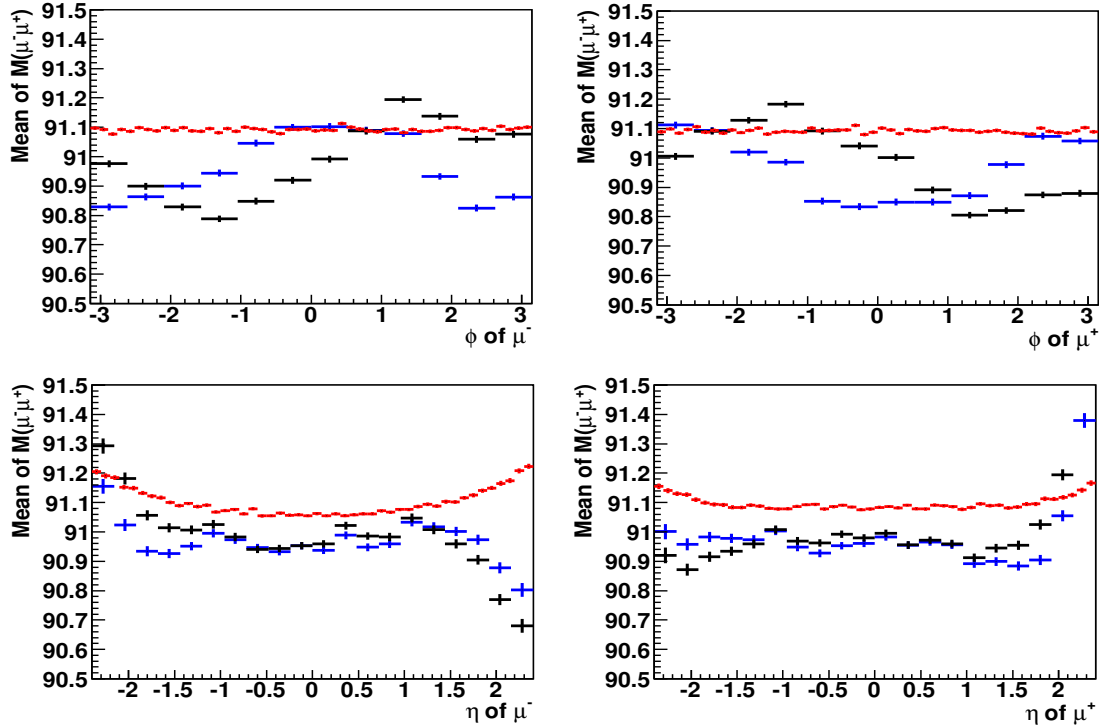


Figure 33: Test of MuscleFit for the first 750 pb^{-1} and $|\eta| < 2.4$: The effect of the MuscleFit correction (for the first 1/3 of the 2011A data) when applied to the same data set used to determine the parameters of the MuscleFit (but only for $|\eta| < 2.1$). Top Plots: Comparison of the average of $M_{\mu\mu}$ as a function of ϕ for μ^- (left) and the average of $M_{\mu\mu}$ as function of ϕ for μ^+ (right) before (black) and after (blue) applying the MuscleFit correction. Bottom Plots: Comparison of the average of $M_{\mu\mu}$ as a function of η for μ^- (left) and the average of $M_{\mu\mu}$ as a function of η for μ^+ (right) before (black) and after (blue) applying the MuscleFit correction. The red points are the $M_{\mu\mu}$ profile plot as a function of ϕ and η for μ^+ and μ^- in the generated level. The average of $M_{\mu\mu}$ is obtained in the tight mass window, $86.5 < M_{\mu\mu} < 96.5 \text{ GeV}/c^2$.

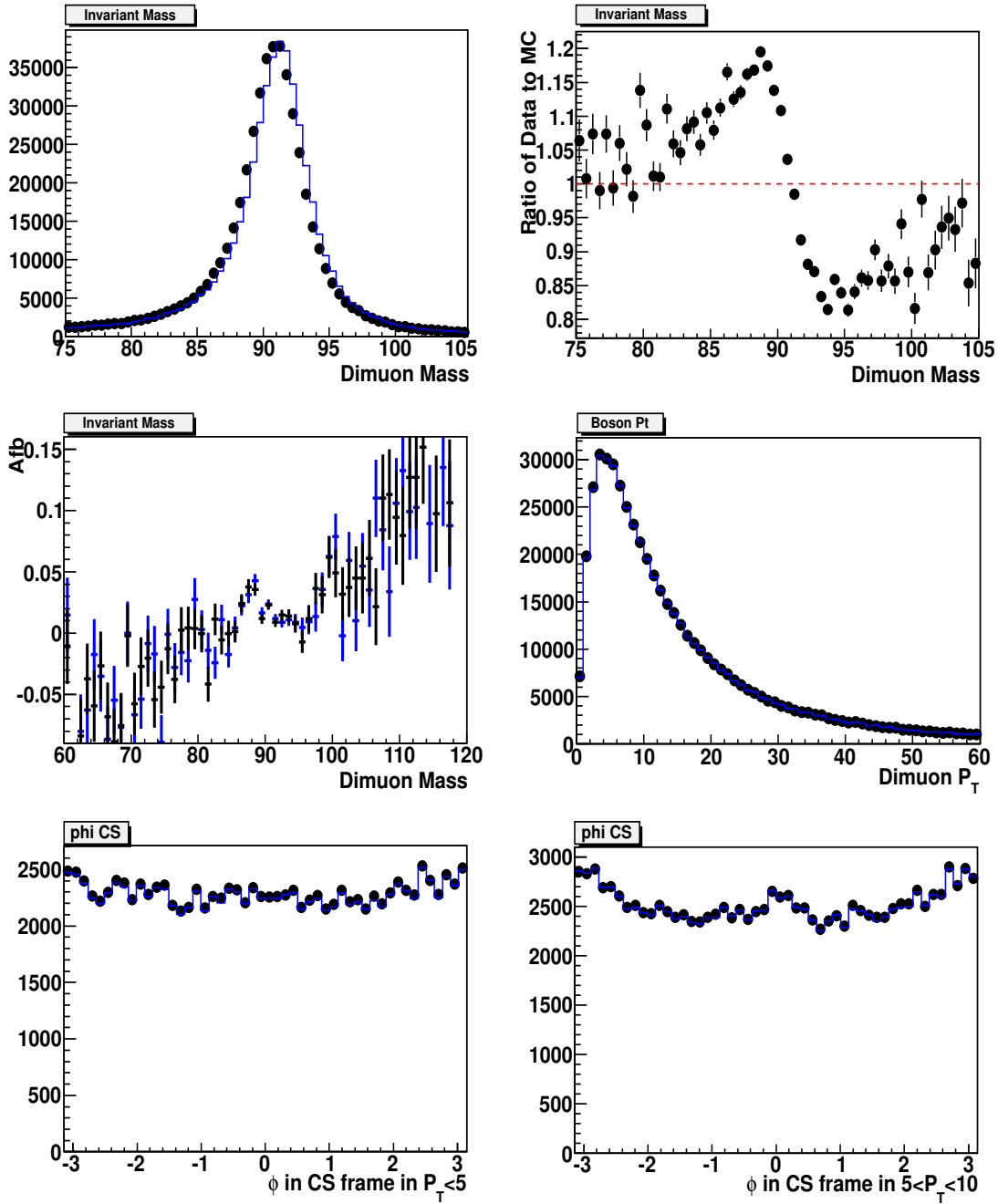


Figure 34: Test of SIDRA for the first 750 pb^{-1} and $|\eta| < 2.4$: The effect of the SIDRA correction (for the first 1/3 of the 2011A data) when applied to the same data set used to determine the parameters of the MuscleFit (but only for $|\eta| < 2.1$) (similar data set as used for SIDRA). Top Plots: Comparison of the dimuon invariant mass distribution before (black) and after (blue) applying SIDRA (left) and its ratio (right). Middle plots: Comparison of A_{fb} (left) and boson P_T (right) distributions before (black) and after (blue) applying SIDRA correction. Bottom plots: Comparison of ϕ in the Collins-Soper frame in boson $P_T < 5 \text{ GeV}/c$ (left) and ϕ in the Collins-Soper frame in boson $5 < P_T < 10 \text{ GeV}/c$ (right) distributions before (black) after (blue) applying the SIDRA correction.

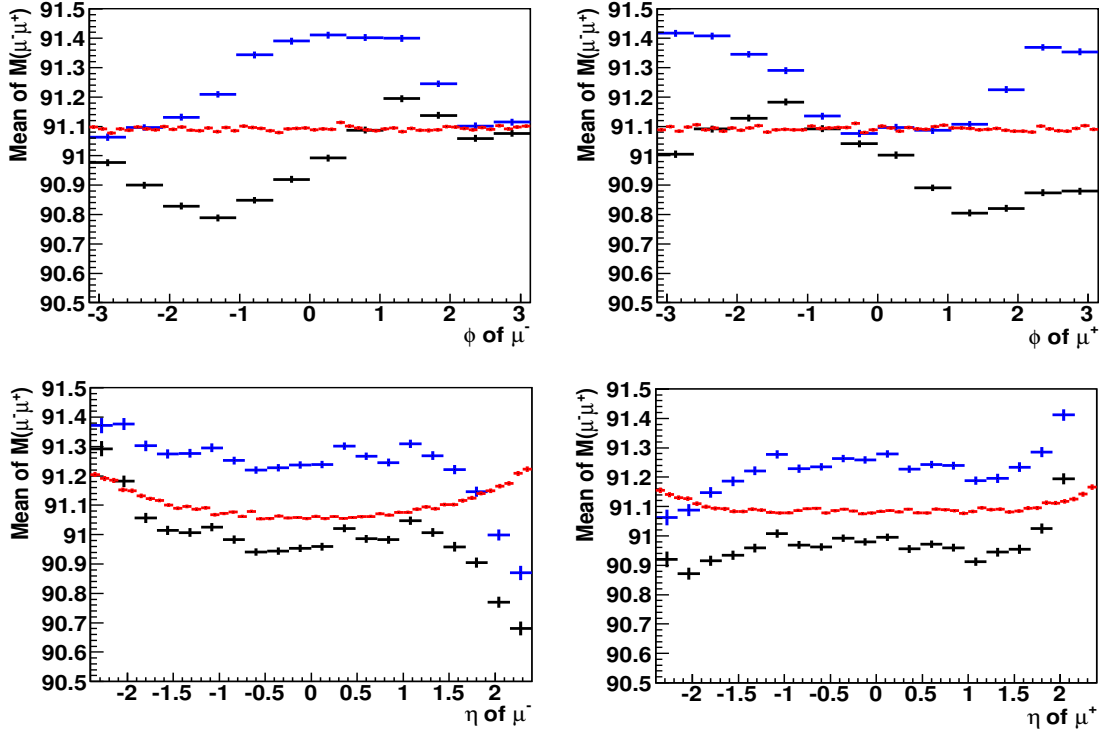


Figure 35: Test of SIDRA for the first 750 pb^{-1} and $|\eta| < 2.4$: The effect of the SIDRA correction (for the first 1/3 of the 2011A data) when applied to the same data set used to determine the parameters of the MuscleFit (but only for $|\eta| < 2.1$) (similar data set as used for SIDRA). Top Plots: Comparison of the average of $M_{\mu\mu}$ as a function of ϕ for μ^- (left) and the average of $M_{\mu\mu}$ as function of ϕ for μ^+ (right) before (black) and after (blue) applying the SIDRA correction. Bottom Plots: Comparison of the average of $M_{\mu\mu}$ as a function of η for μ^- (left) and the average of $M_{\mu\mu}$ as a function of η for μ^+ (right) before (black) and after (blue) applying the SIDRA correction. The red points are the $M_{\mu\mu}$ profile plot as a function of ϕ and η for μ^+ and μ^- in the generated level. The average of $M_{\mu\mu}$ is obtained in the tight mass window, $86.5 < M_{\mu\mu} < 96.5 \text{ GeV}/c^2$.

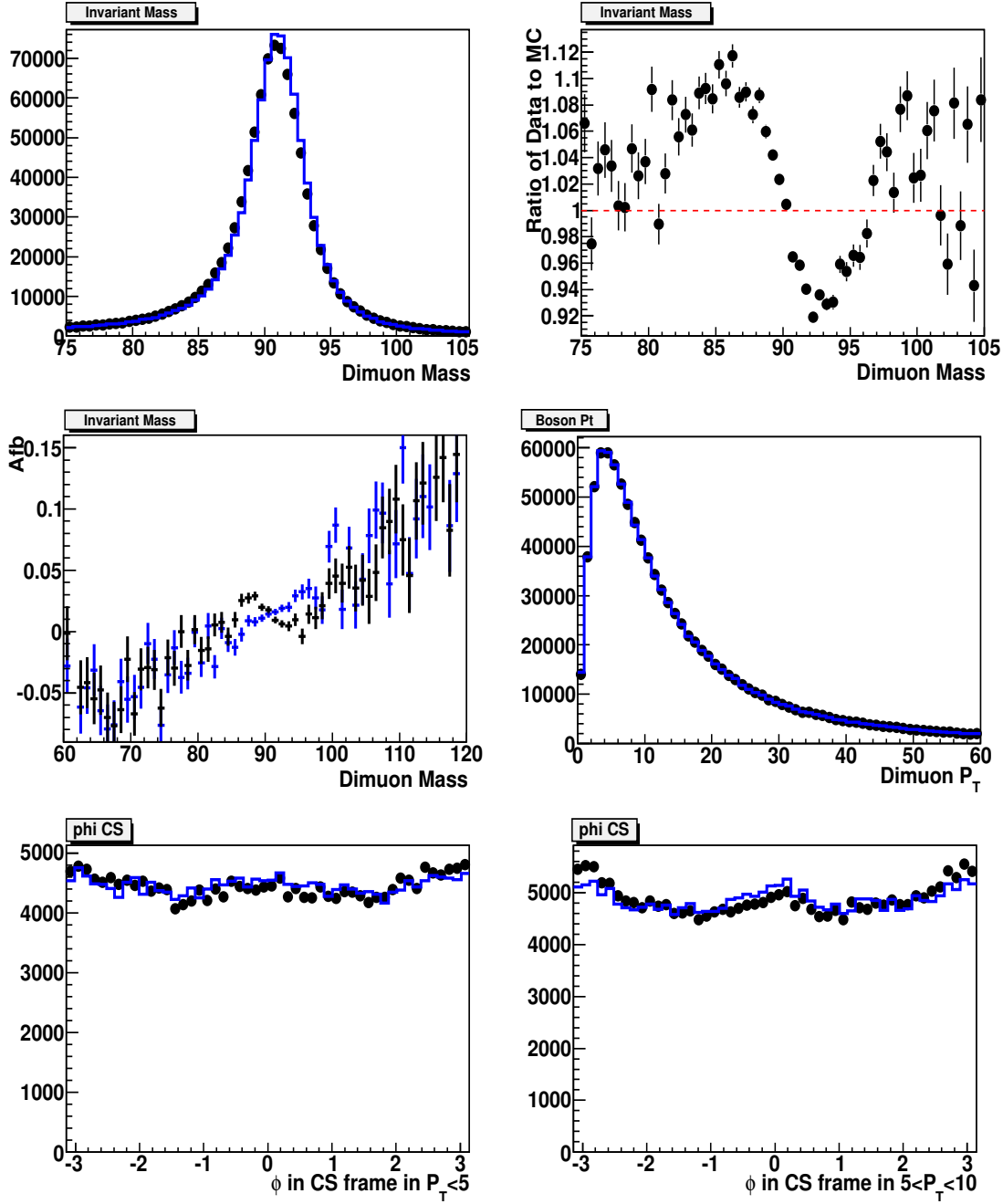


Figure 36: Test of our Rochester correction for the 2011A 2.1 fb^{-1} data with $|\eta| < 2.4$: The effect of the Rochester correction when applied to the data. Top Plots: Comparison of the dimuon invariant mass distribution before (black) and after (blue) applying the Rochester correction (left) and its ratio (right). Middle plots: Comparison of A_{fb} (left) and boson P_T (right) distributions before (black) and after (blue) applying the Rochester correction. Bottom plots: Comparison of ϕ in the Collins-Soper frame in boson $P_T < 5 \text{ GeV}/c$ (left) and ϕ in the Collins-Soper frame in boson $5 < P_T < 10 \text{ GeV}/c$ (right) distributions before (black) after (blue) applying the Rochester correction.

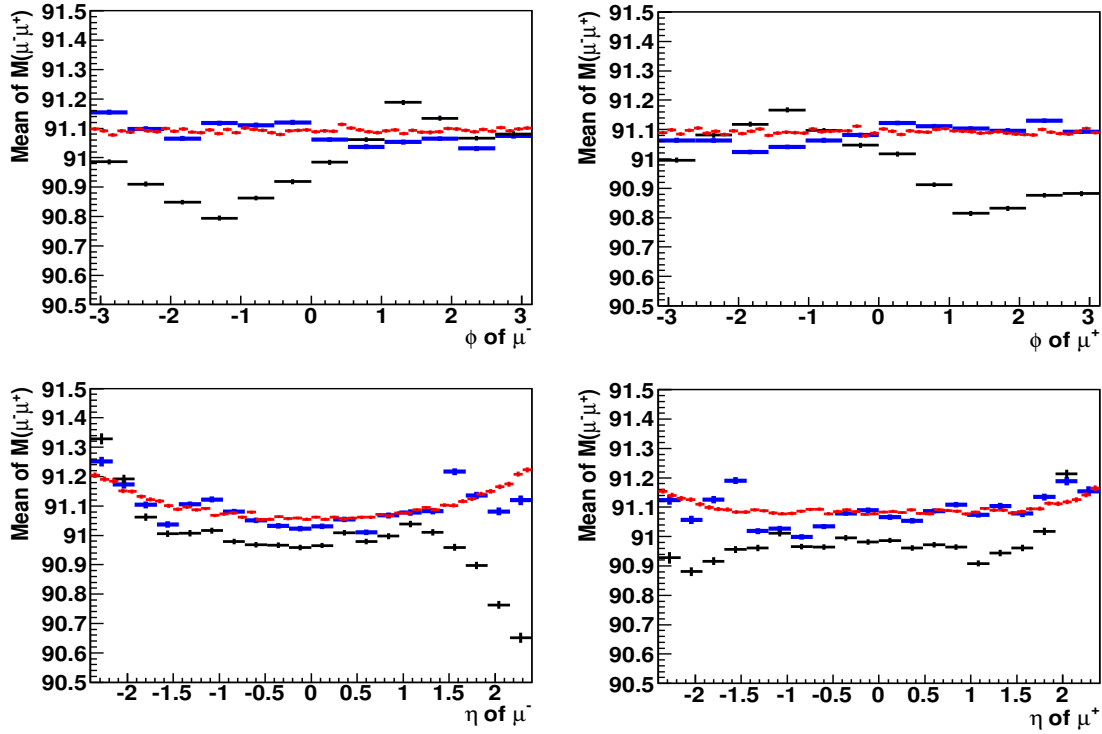


Figure 37: Test of our Rochester correction for the 2011A 2.1 fb^{-1} data with $|\eta| < 2.4$: The effect of the Rochester correction when applied to the data. Top Plots: Comparison of the average of $M_{\mu\mu}$ as a function of ϕ for μ^- (left) and the average of $M_{\mu\mu}$ as function of ϕ for μ^+ (right) before (black) and after (blue) applying the Rochester correction. Bottom Plots: Comparison of the average of $M_{\mu\mu}$ as a function of η for μ^- (left) and the average of $M_{\mu\mu}$ as a function of η for μ^+ (right) before (black) and after (blue) applying the Rochester correction. The red points are the $M_{\mu\mu}$ profile plot as a function of ϕ and η for μ^+ and μ^- in the generated level. The average of $M_{\mu\mu}$ is obtained in the tight mass window, $86.5 < M_{\mu\mu} < 96.5 \text{ GeV}/c^2$.

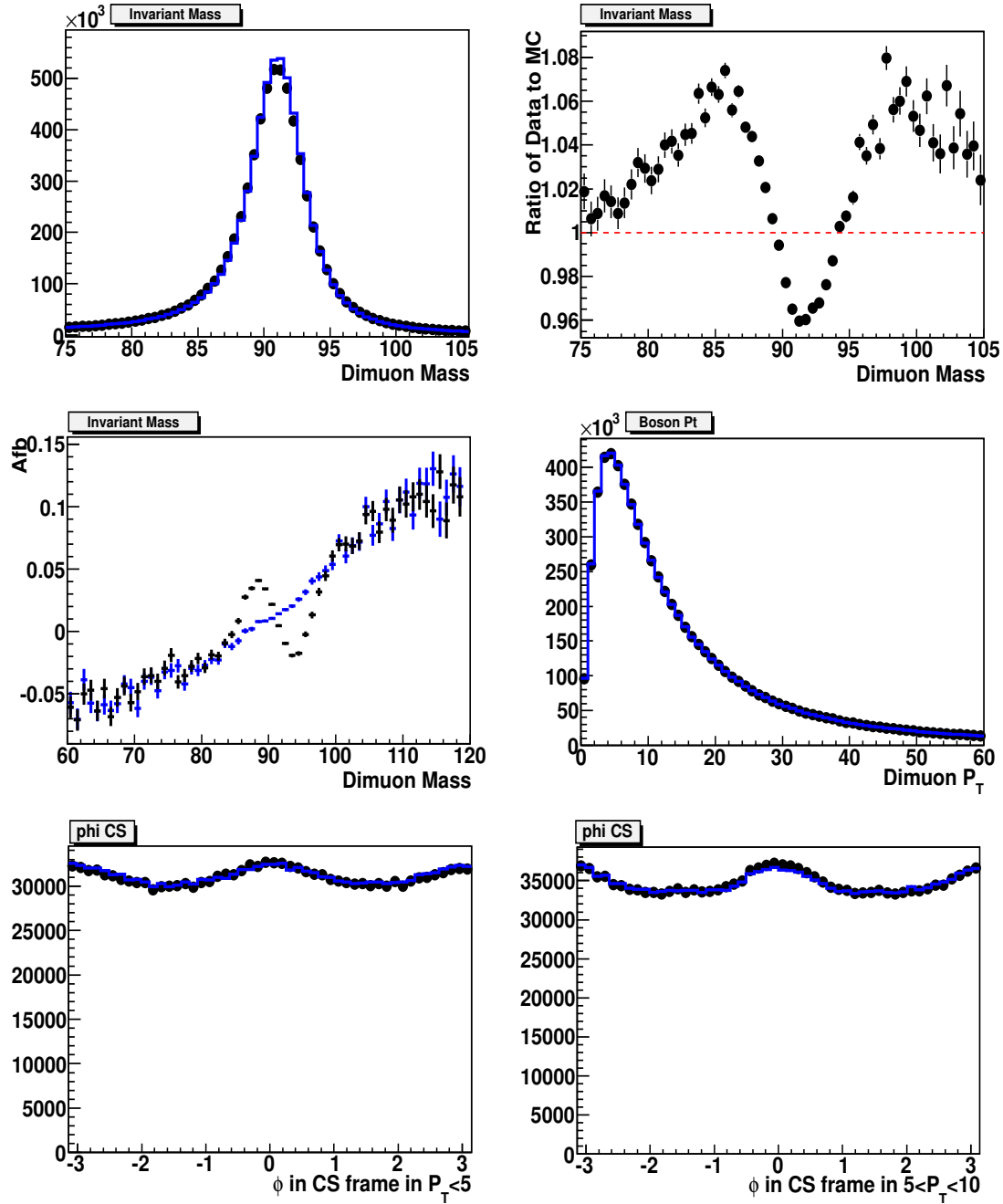


Figure 38: Test of four Rochester correction for the 2011A MC (Summer 2011) with $|\eta| < 2.4$: The effect of the Rochester correction when applied to MC. Top Plots: Comparison of the dimuon invariant mass distribution before (black) and after (blue) applying the Rochester correction (left) and its ratio (right). Middle plots: Comparison of A_{fb} (left) and boson P_T (right) distributions before (black) and after (blue) applying the Rochester correction. Bottom plots: Comparison of ϕ in the Collins-Soper frame in boson $P_T < 5 \text{ GeV}/c$ (left) and ϕ in the Collins-Soper frame in boson $5 < P_T < 10 \text{ GeV}/c$ (right) distributions before (black) after (blue) applying the Rochester correction.

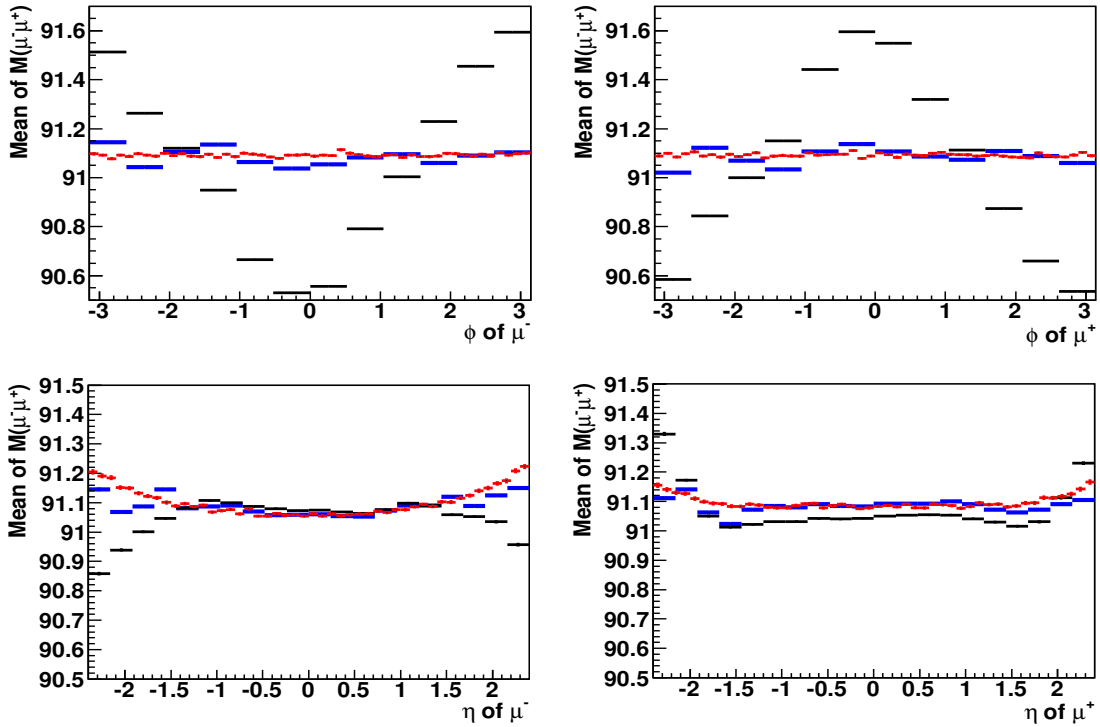


Figure 39: Test of our Rochester correction for 2011A MC (Summer 2011) with $|\eta| < 2.4$: The effect of the Rochester correction when applied to MC. Top Plots: Comparison of the average of $M_{\mu\mu}$ as a function of ϕ for μ^- (left) and the average of $M_{\mu\mu}$ as function of ϕ for μ^+ (right) before (black) and after (blue) applying the Rochester correction. Bottom Plots: Comparison of the average of $M_{\mu\mu}$ as a function of η for μ^- (left) and the average of $M_{\mu\mu}$ as a function of η for μ^+ (right) before (black) and after (blue) applying the Rochester correction. The red points are the $M_{\mu\mu}$ profile plot as a function of ϕ and η for μ^+ and μ^- in the generated level. The average of $M_{\mu\mu}$ is obtained in the tight mass window, $86.5 < M_{\mu\mu} < 96.5 \text{ GeV}/c^2$.

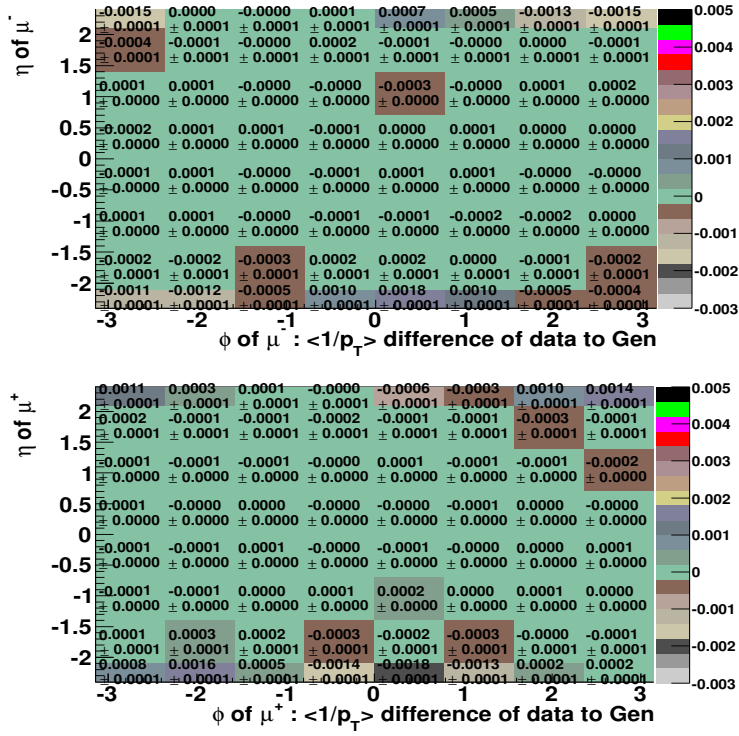


Figure 40: Incremental Rochester correction for MuscleFit: The $\langle 1/p_T \rangle$ correction for 2011A data to be used on top of MuscleFit for μ^- (top) and μ^+ (bottom) in η and ϕ .

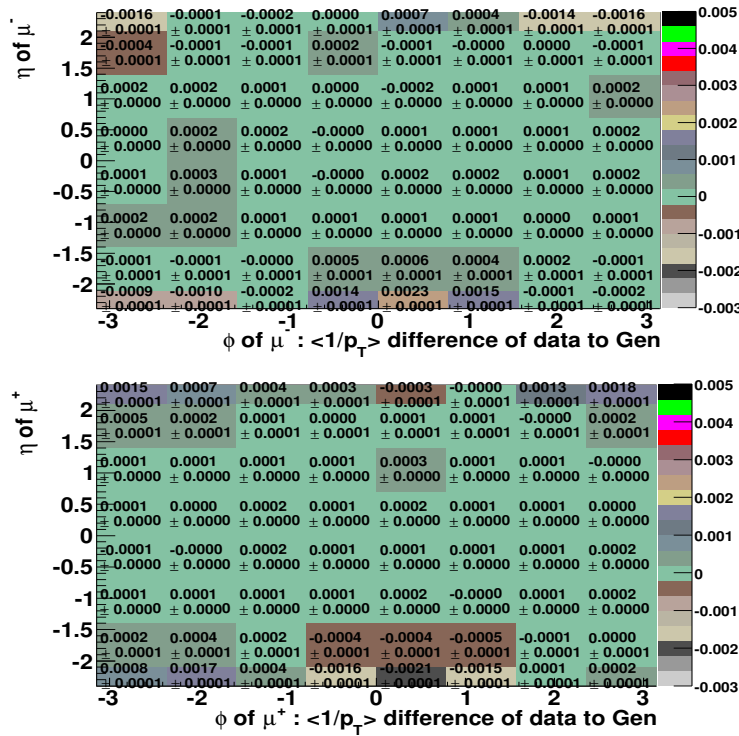


Figure 41: Incremental Rochester correction for SIDRA: The $\langle 1/p_T \rangle$ correction for 2011A data to be used on top of SIDRA correction for μ^- (top) and μ^+ (bottom) in η and ϕ .

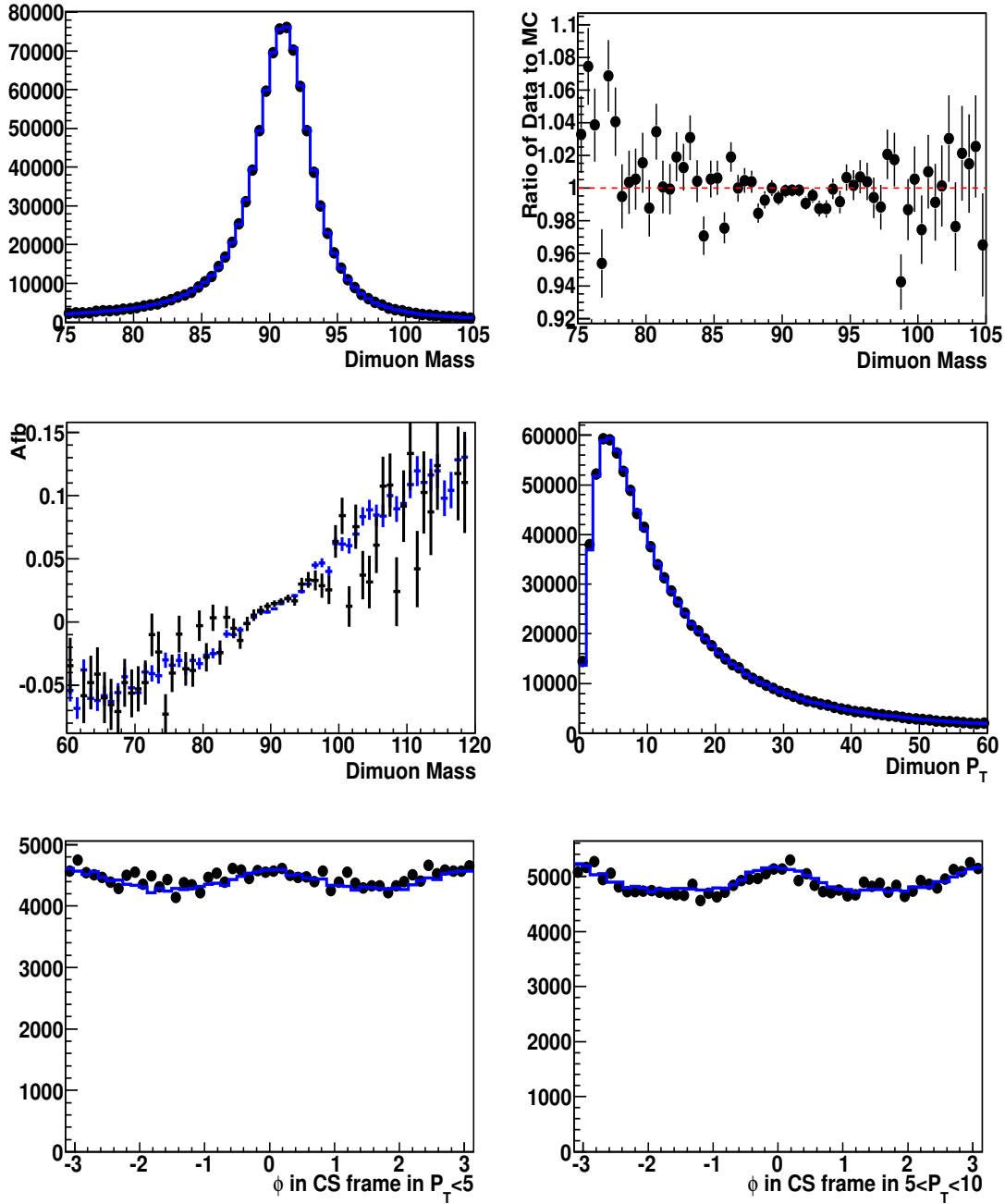


Figure 42: The reference plots ($M_{\mu^+\mu^-}$, A_{fb} , $Z P_T$, and ϕ_{CS}) after the application of the Rochester incremental muon momentum correction on top of MuscleFit for the 2011A (2.1 fb^{-1}) data vs. the 2011A MC (corrected for with the full Rochester correction). Top Plots: Comparison of the dimuon invariant mass distribution between the data (black) and MC (blue) (left) and its ratio of data to MC (right). Middle plots: Comparison of A_{fb} (left) and boson P_T (right) distributions between the data (black) and MC (blue). Bottom plots: Comparison of ϕ in the Collins-Soper frame in boson $P_T < 5 \text{ GeV}/c$ (left) and ϕ in the Collins-Soper frame in boson $5 < P_T < 10 \text{ GeV}/c$ (right) distributions between the data (black) and MC (blue). The plots are normalized to the total number of events of the data in $60 < M_{\mu\mu} < 120 \text{ GeV}/c^2$.

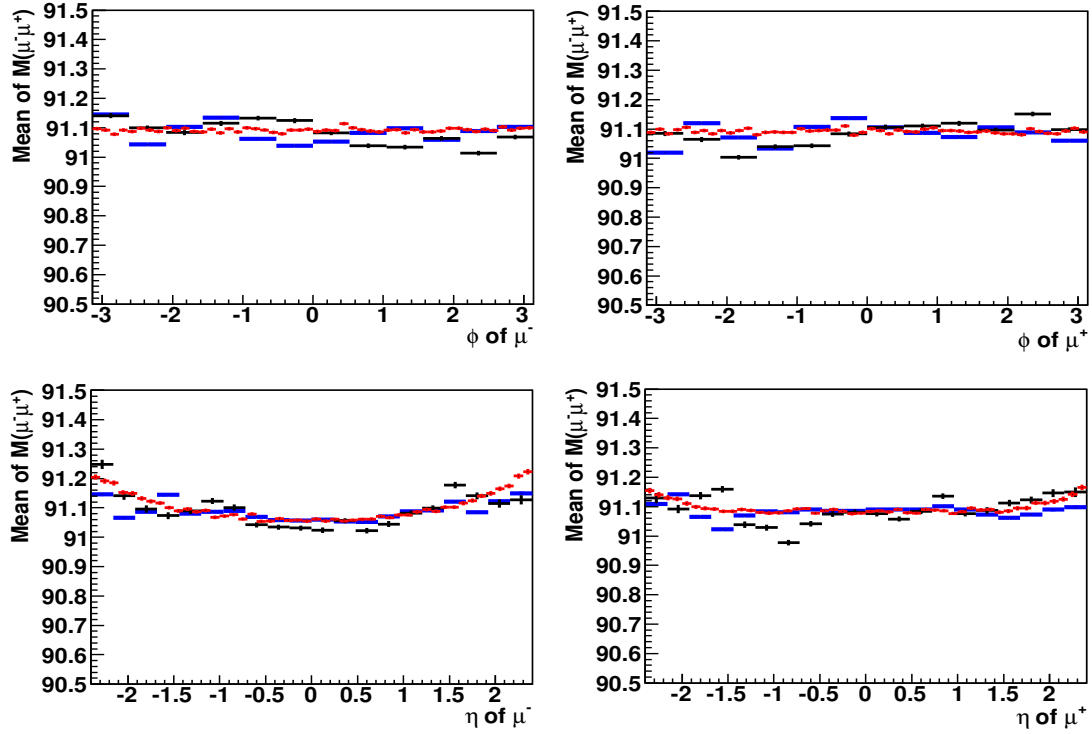


Figure 43: The $M_{\mu^+\mu^-}$ profile plot as a function of η and ϕ of μ^+ and μ^- after the Rochester incremental muon momentum correction on top of MuscleFit for the 2011A (2.1 fb^{-1}) data vs. the 2011A MC (corrected for with the full Rochester correction). Top Plots: Comparison of the average of $M_{\mu\mu}$ in ϕ of μ^- (left) and the average of $M_{\mu\mu}$ in ϕ of μ^+ (right) between the data (black) and MC (blue). Bottom Plots: Comparison of the average of $M_{\mu\mu}$ in η of μ^- (left) and the average of $M_{\mu\mu}$ in η of μ^+ (right) between the data (black) and MC (blue). The red points are the $M_{\mu\mu}$ profile plot as a function of ϕ and η for μ^+ and μ^- . The average of $M_{\mu\mu}$ is obtained in the Z peak region, $86.5 < M_{\mu\mu} < 96.5 \text{ GeV}/c^2$.

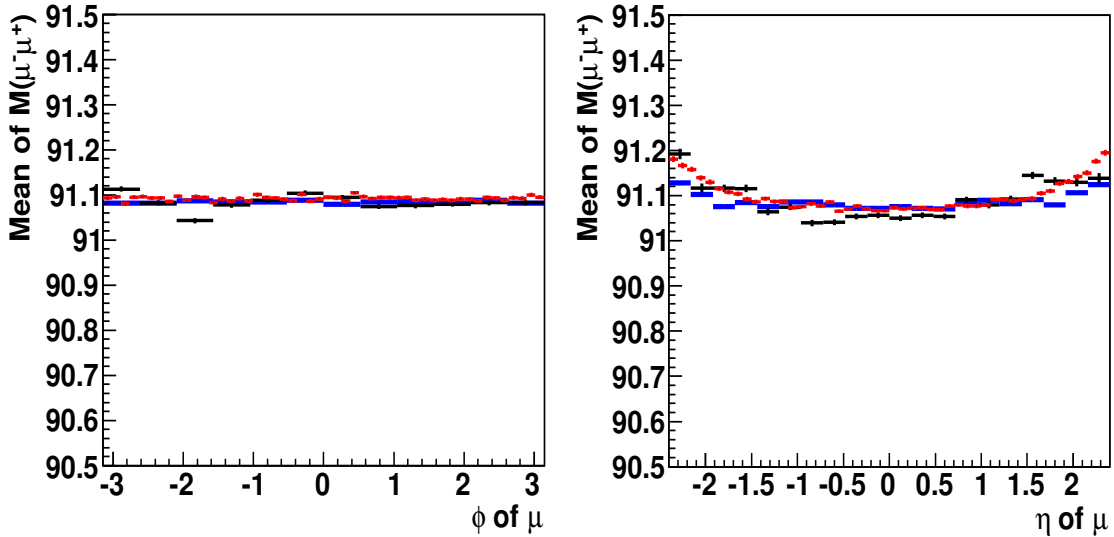


Figure 44: The $M_{\mu^+\mu^-}$ profile plot as a function of ϕ (left) and η (right) of μ (no charge requirement) after applying the Rochester incremental muon momentum correction on top of MuscleFit for the 2011A (2.1 fb^{-1}) data vs. the 2011A MC (corrected for with the full Rochester correction). The average of $M_{\mu\mu}$ is obtained in the Z peak region, $86.5 < M_{\mu\mu} < 96.5 \text{ GeV}/c^2$.

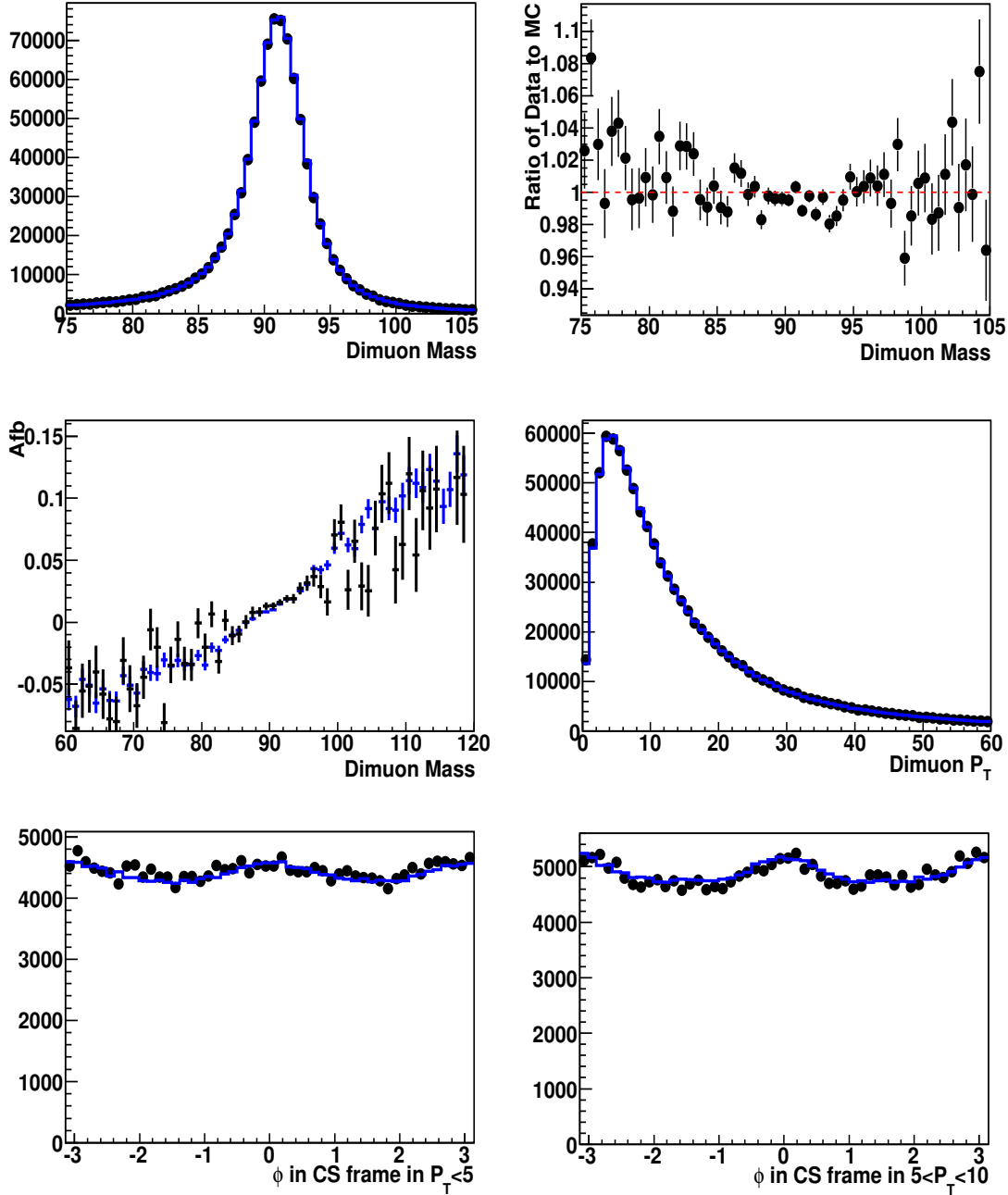


Figure 45: The reference plots ($M_{\mu^+\mu^-}$, A_{fb} , $Z P_T$, and ϕ_{CS}) after the application of the Rochester incremental muon momentum correction on top of SIDRA for the 2011A (2.1 fb^{-1}) data vs. the 2011A MC (corrected for with the full Rochester correction). Top Plots: Comparison of the dimuon invariant mass distribution between the data (black) and MC (blue) (left) and its ratio of data to MC (right). Middle plots: Comparison of A_{fb} (left) and boson P_T (right) distributions between the data (black) and MC (blue). Bottom plots: Comparison of ϕ in the Collins-Soper frame in boson $P_T < 5 \text{ GeV}/c$ (left) and ϕ in the Collins-Soper frame in boson $5 < P_T < 10 \text{ GeV}/c$ (right) distributions between the data (black) and MC (blue). The plots are normalized to the total number of events of the data in $60 < M_{\mu\mu} < 120 \text{ GeV}/c^2$.

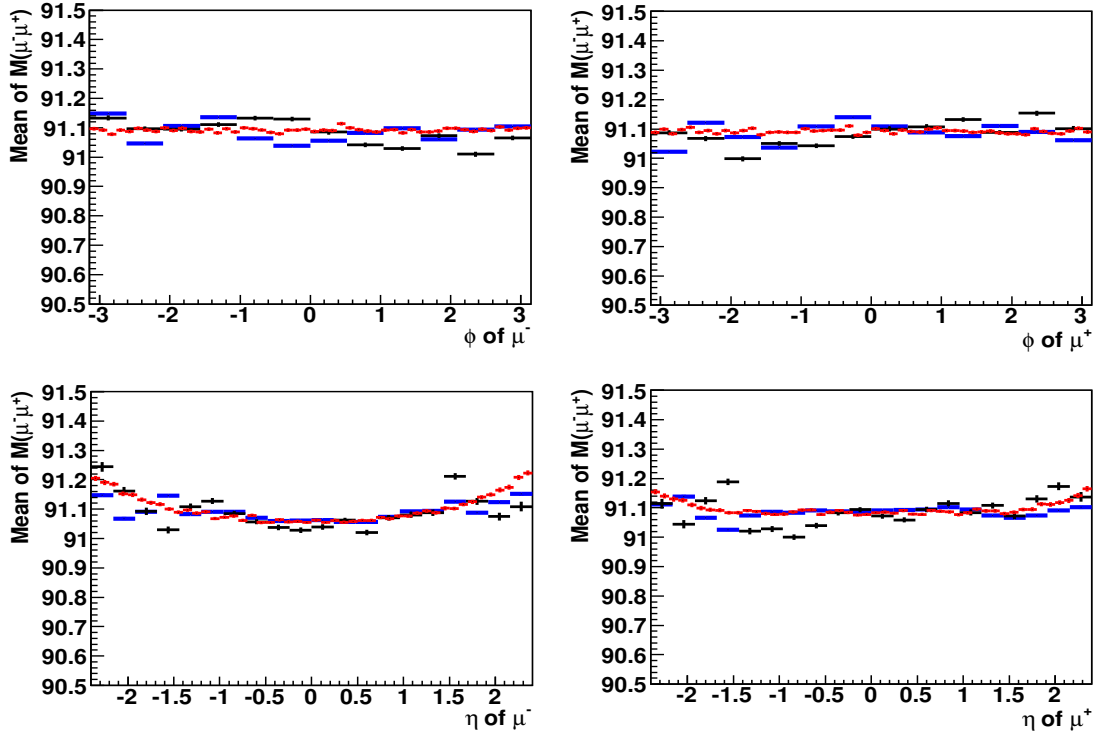


Figure 46: The $M_{\mu^+\mu^-}$ profile plot as a function of η and ϕ of μ^+ and μ^- after the Rochester incremental muon momentum correction on top of SIDRA for the 2011A (2.1 fb^{-1}) data vs. the 2011A MC (corrected for with the full Rochester correction). Top Plots: Comparison of the average of $M_{\mu\mu}$ in ϕ of μ^- (left) and the average of $M_{\mu\mu}$ in ϕ of μ^+ (right) between the data (black) and MC (blue). Bottom Plots: Comparison of the average of $M_{\mu\mu}$ in η of μ^- (left) and the average of $M_{\mu\mu}$ in η of μ^+ (right) between the data (black) and MC (blue). The red points are the $M_{\mu\mu}$ profile plot as a function of ϕ and η for μ^+ and μ^- . The average of $M_{\mu\mu}$ is obtained in the Z peak region, $86.5 < M_{\mu\mu} < 96.5 \text{ GeV}/c^2$.

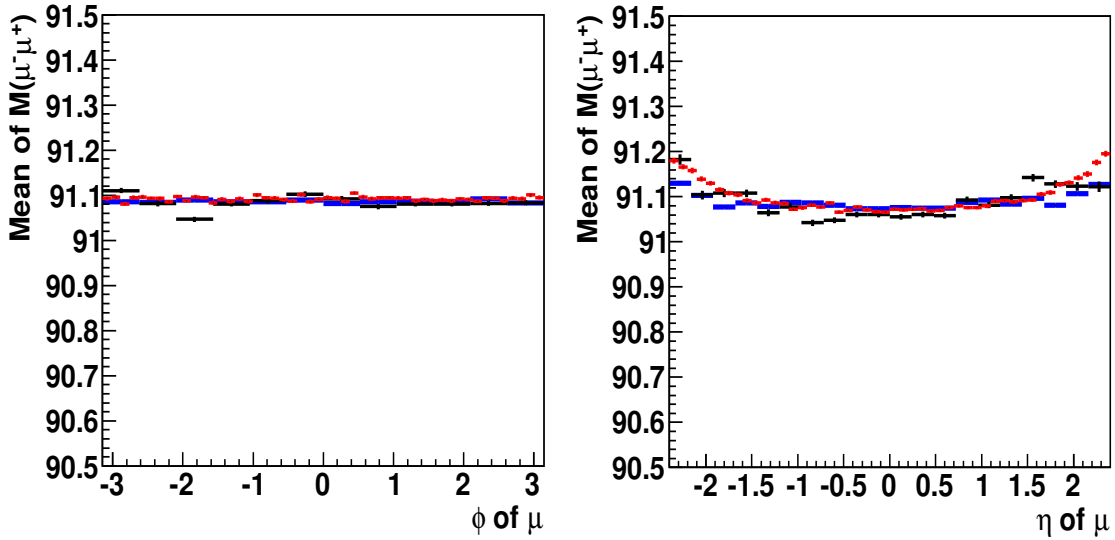


Figure 47: The $M_{\mu^+\mu^-}$ profile plot as a function of ϕ (left) and η (right) of μ (no charge requirement) after applying the Rochester incremental muon momentum correction on top of SIDRA for the 2011A (2.1 fb^{-1}) data vs. the 2011A MC (corrected for with the full Rochester correction). The average of $M_{\mu\mu}$ is obtained in the Z peak region, $86.5 < M_{\mu\mu} < 96.5 \text{ GeV}/c^2$.

Table 3: Additional resolution parameters (Δ , and SF) to be applied to the 2011A MC to match to the data for which the Rochester incremental correction is applied on top of MuscleFit or SIDRA correction. These parameters are determined by comparing the $M_{\mu^+\mu^-}$ distributions in data and MC. The global scale factors G^{data} and G^{MC} are used to set the Z peak position at the correct place.

Global Factor	MuscleFit	SIDRA
Δ	$(-2.8958 \pm 0.7867) \times 10^{-6}$	$(-3.4600 \pm 0.7728) \times 10^{-6}$
SF	44.3096 ± 1.6643	40.2147 ± 1.3409
G^{data}	1.0009 ± 0.0001	1.0012 ± 0.0001
G^{MC}	1.0000 ± 0.0001	1.0000 ± 0.0001

- 362 [2] SIDRA for 2011A data set : Presentation in CMS Muon POG Meeting (August. 8th, 2011). The presentation
363 is linked at [https://indico.cern.ch/getFile.py/access?contribId=2&resId=0&materialId=](https://indico.cern.ch/getFile.py/access?contribId=2&resId=0&materialId=slides&confId=128974)
364 [slides&confId=128974](https://indico.cern.ch/getFile.py/access?contribId=2&resId=0&materialId=slides&confId=128974).
- 365 [3] For the most recent version of POWHEG. See Simone Alioli, Paolo Nason, Carlo Oleari, Emanuele Re,
366 arXiv:1009.5594v1 (2010). earlier versions are discussed in JHEP 0807:060,2008. NSF-KITP-08-74, May
367 2008. 35pp. e-Print: arXiv:0805.4802 [hep-ph]
- 368 [4] J. C. Collins and D. E. Soper, Phys. Rev. D **16**, 2219 (1977). The CS frame is the center of mass of the γ^*/Z ,
369 where the z axis is defined as the bisector of the p and \bar{p} beams. The polar angle is defined as the angle of the
370 positive lepton with respect to the proton direction.
- 371 [5] CMS collaboration, “Search for Resonances in the Dimuon Mass Distribution in pp collisions at $\sqrt{s} = 7$ TeV”,
372 CMS PAS EXO-10-013 (2010).
- 373 [6] J.G., G.P., D.G., K.K., N.K. (Northeastern University), “Measurement of the $Z/\gamma^* \rightarrow \mu^+\mu^-$ transverse mo-
374 mentum distribution in pp collisions at $\sqrt{s} = 7$ TeV”, CMS note - Archive ID: 30523M